

## Original Research Communication

**Nitrosopersulfide (SSNO<sup>-</sup>) is a unique cysteine polysulfidating agent with reduction-resistant bioactivity**

Virág Bogdándi<sup>1</sup>, Tamás Ditrói<sup>1</sup>, István Zoárd Batai<sup>2</sup>, Zoltán Sándor<sup>2</sup>, Magdalena Minnion<sup>3</sup>, Anita Vasas<sup>1,4</sup>, Klaudia Galambos<sup>1</sup>, Péter Buglyó<sup>4</sup>, Erika Pintér<sup>2</sup>, Martin Feelisch<sup>3</sup> and Péter Nagy<sup>1\*</sup>

<sup>1</sup>*Department of Molecular Immunology and Toxicology, National Institute of Oncology, Ráth György utca 7-9, Budapest, Hungary, 1122*

<sup>2</sup>*Department of Pharmacology and Pharmacotherapy, Medical School, University of Pécs, Pécs, Hungary*

<sup>3</sup>*Clinical and Experimental Sciences, Faculty of Medicine, and University Hospital Southampton NHS Foundation Trust, University of Southampton, Southampton SO16 6YD, United Kingdom.*

<sup>4</sup>*Department of Inorganic and Analytical Chemistry, University of Debrecen, Egyetem tér 1, Debrecen, Hungary, 4010*

**Running Head:** Sustained SSNO<sup>-</sup> induced polysulfidation

Corresponding author: Department of Molecular Immunology and Toxicology, National Institute of Oncology, Ráth György utca 7-9, 1122 Budapest, Hungary; peter.nagy@oncol.hu; Tel. +36-1-224-8600/3644

Word count: 7903 (excluding references and figure legends)

Reference numbers: 31

Number of color illustrations: 8 (plus 2 supplementary figures)

Manuscript keywords: nitric oxide, hydrogen sulfide, persulfidation, redox-signaling, TRPA1

## Abstract

**Aims:** The aim of the present study was to investigate the biochemical properties of nitrosopersulfide ( $\text{SSNO}^-$ ), a key intermediate of the NO/sulfide crosstalk.

**Results:** We obtained corroborating evidence that  $\text{SSNO}^-$  is indeed a major product of the reaction of S-nitrosothiols with  $\text{H}_2\text{S}$ . It was found to be relatively stable ( $t_{1/2} \sim 1\text{h}$  at RT) in aqueous solution of physiological pH, stabilized by the presence of excess sulfide and resistant towards reduction by other thiols. Furthermore, we here show that  $\text{SSNO}^-$  escapes the reducing power of the NADPH-driven biological reducing machineries, the thioredoxin and glutathione reductase systems. The slow decomposition of  $\text{SSNO}^-$  produces inorganic polysulfide species, which effectively induce per/polysulfidation on glutathione or protein Cys residues. Our data also demonstrate that, in contrast to the transient activation by inorganic polysulfides,  $\text{SSNO}^-$  induces long-term potentiation of TRPA1 channels, which may be due to its propensity to generate a slow flux of polysulfide *in situ*.

**Innovation:** The characterized properties of  $\text{SSNO}^-$  would seem to represent unique features in cell signaling by enabling sulfur and nitrogen trafficking within the reducing environment of the cytosol, with targeted release of both NO and polysulfide equivalents.

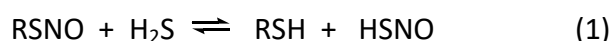
**Conclusion:**  $\text{SSNO}^-$  is a surprisingly stable bioactive product of the chemical interaction of S-nitrosothiol species and  $\text{H}_2\text{S}$  that is resistant to reduction by the thioredoxin and glutathione systems. As well as generating NO, it releases inorganic polysulfides, enabling transfer of sulfane-sulfur species to peptide/proteine Cys residues. The sustained activation of TRPA1 channels by  $\text{SSNO}^-$  is most likely linked to all these properties.

## Introduction

Following the discoveries of nitric-oxide (NO) and carbon-monoxide (CO) as small endogenously produced signaling molecules, hydrogen sulfide (H<sub>2</sub>S) has emerged as the “new kid on the block” with an even wider-ranging array of biological actions compared to the former two entities (1,30,33,38-40). Cooperative effects between NO and H<sub>2</sub>S were first observed by Kimura and colleagues, raising the possibility of a cross-talk between their mediator functions (20). Several elegant studies since then contributed to accumulate further evidence for the reciprocal regulation of NO and sulfide biosynthetic pathways and the mutually cooperative nature of interaction at the level of cell signaling (23). Furthermore, as their biosynthetic machineries are often co-localized in a variety of cells and tissues, the potential for chemical interaction to produce secondary bioactive products has become an increasingly attractive field of investigation; those research activities will likely uncover many new layers of regulatory processes in redox biology in the near future. To conceptualize the chemical and functional interactions of NO and H<sub>2</sub>S-derived Reactive Nitrogen Species and Reactive Sulfur Species with the long-studied Reactive Oxygen Species we recently introduced the concept of the ‘Reactive Species Interactome’ (RSI) (10,12). The RSI represents the biochemical sensing and adaptation system that enables individual cells (and entire organisms) to adjust their metabolic machinery to changes in demand or environmental conditions to stay ‘fit for purpose’. To this end, sulfur-nitrogen compounds likely play a fundamental role in enabling survival.

In their earlier studies, Whiteman et al. proposed the formation of thionitrous acid (HSNO), the smallest possible nitrosothiol, as a central intermediate in the chemical interactions of NO with sulfide species (43). Filipovic and co-workers later claimed that the reactions between S-nitrosothiols (RSNO) and sulfide give rise to the formation of HSNO; the authors proposed that HSNO is relatively stable (under physiological conditions the suggested half-life was 30 min) and acts as a source of NO<sup>+</sup>, NO<sup>•</sup> and NO<sup>-</sup>, with the potential to support intracellular transnitrosation events (18). On the contrary, we and others argued that this compound is rather unstable ( $t_{1/2} \sim 6$ s measured by Filipovic et al themselves in ref (18)) and undergoes rapid isomerization, homolysis and polymerization reactions, questioning its ability to serve as a central molecule in regulating intracellular

signaling events (9,26,28). Moreover, accumulating evidence demonstrated that the direct chemical interactions between NO donors and H<sub>2</sub>S result in a network of cascading chemical reactions, with the generation of a plethora of bioactive molecules including nitrosopersulfide (SSNO<sup>-</sup>), sulfite (SO<sub>3</sub><sup>-</sup>), dinitrososulfite (SULFI/NO) and inorganic polysulfides (11). We demonstrated that SSNO<sup>-</sup> formation during the reactions of nitrosothiols with sulfide is a process in which *in situ* generated inorganic polysulfides serve as autocatalysts.



Compounds in reactions 1-4 are depicted in their fully protonated states for the sake of simplicity, but they represent all acid/base derivative.

Cys-per/polysulfide species were shown by a number of different research groups using different methods to be abundant in biological systems (2,14,15,19,21,32,45). Cys-polysulfides are in dynamic equilibrium with inorganic polysulfide species (6), which implies that their reactions with nitrosothiols could be a potential source of endogenous SSNO<sup>-</sup>. In addition, it was also shown to be generated in the chemical interactions of sulfide and persulfides with nitrite, representing another potential source of endogenous SSNO<sup>-</sup> (4,8).

The early studies on SSNO<sup>-</sup> triggered lively debates on chemical grounds (4,7,22,27,41). For example, Wedmann et al. claimed that SSNO<sup>-</sup> was unstable and rapidly decomposed in the presence of thiols or cyanide. However, the kinetic measurements with different nucleophiles were performed in organic solvents or in mixtures of aqueous and organic solvents using PNP<sup>+</sup>SSNO<sup>-</sup> as a reagent (which is inhomogenous and contains substantial uncharacterized chemical entities, likely affecting its stability). Conversely, we and others provided robust evidence for the notion that SSNO<sup>-</sup> has considerable stability under physiological conditions and is resistant to thiols (such as dithiotreitol (DTT) or reduced glutathione (GSH)) and cyanide (4,9,11,26,28). These findings are corroborated by

several experiments in the present contribution, and we propose that the main reason for these conflicting observations lies in methodological details of preparing and working with  $SSNO^-$  solutions and misinterpretations in ref (42) by e.g. missing the 420 nm band being due to  $SSNO^-$  (related to a solvatochromic effect, also addressed by Pluth et al (4)), as well as erroneous assignment of the aqueous 314 ppm signal to  $SNO^-$ , whereas it really pertains to  $SSNO^-$  (27)

The central aim of the current study was to further investigate the chemical properties of  $SSNO^-$  in relation to its potential biological actions. Importantly, we here demonstrate that contrary to other polysulfide species,  $SSNO^-$  exhibits unexpected resistance towards the main NADPH-driven biological reducing machineries, the thioredoxin (TrxR) and the glutathione reductase (GR) systems. Furthermore, we now obtained mass spectrometric evidence that its slow decomposition gives rise to the formation of inorganic polysulfides, which in turn induce rapid per- and polysulfidation of peptide and protein cysteine residues. Transient receptor potential ankyrin 1 (TRPA1) channels were previously proposed to be activated by inorganic polysulfides via persulfidation of their critical regulatory cysteine (Cys) residues (24). The cooperative actions of sulfide and NO on TRPA1 channel activation had been proposed earlier to be mediated via intermediate formation of nitroxyl (HNO) (16). On the contrary, Kimura and co-workers recently demonstrated that these effects are rather due to inorganic polysulfides arising as products of the chemical interaction between NO and sulfide (25). Here we show that not only the rapidly generated inorganic polysulfides (that form concomitantly with  $SSNO^-$  during the chemical reaction of nitrosothiols and sulfide (11)) can activate TRPA1 channels, but the slow release of these molecules upon  $SSNO^-$  decomposition can sustain their activation status. Because contrary to polysulfides,  $SSNO^-$  can escape the NADPH-driven reducing systems, we propose that its localized decomposition provides a slow *in situ* flux of sulfane sulfur species that sustains TRPA1 activation. These observations represent an example as to how the chemical interactions of reactive species in the NO and sulfide regulatory pathways can result in additional biological activities not entertained by either signaling entities alone. These observations

make  $SSNO^-$  a highly attractive candidate molecule for intra- and possibly intercellular trafficking of NO and sulfane sulfur equivalents.

## Results and Discussion

*Corroborating evidence for the formation of  $SSNO^-$  as a major product in the reaction of nitrosothiols with  $H_2S$  and for its stability in the presence of thiols*

$SSNO^-$  was first characterized in the 1980s by Seel and Wagner in the form of its bis(triphenylphosphine)iminium salt ( $PNP^+SSNO^-$ ). The chemical structure of the anion was determined by X-ray crystallography and its UV-vis spectrum was recorded in different organic solvents (35). The absorbance maxima of  $SSNO^-$  in acetone and methanol were at 448 nm and 426 nm, respectively, with a calculated molar absorbance coefficient of 2800  $M^{-1}cm^{-1}$  in acetone. Previously, we reported the formation of a yellow product with a peak at  $\lambda_{max} = 412$  nm (denominated as the '412 species'), with a molar absorbance coefficient of 6000  $M^{-1}cm^{-1}$  that was generated in the reaction of S-nitrosothiols with  $H_2S$  in buffered aqueous solution. Based on high-resolution mass spectrometry data and a number of indirect experimental results (release of NO and sulfide under reducing conditions or sulfane sulfur equivalents under non-reducing conditions) we tentatively assigned this yellow product to  $SSNO^-$  (9,11). Our data suggested that  $SSNO^-$  (the '412 species') was relatively stable at room temperature and physiological pH and slowly decomposed ( $t_{1/2} \sim 0.5$ -1h, depending on conditions) with concomitant formation of NO and sulfane sulfur species. In addition, cell based and *in vivo* data suggested that it could be one of the key bioactive intermediates of the chemical interaction between sulfide and NO that has a relatively long lifetime (on the order of tens of minutes rather than seconds). Notwithstanding these findings and Seel's earlier work, Filipovic and co-workers claimed that  $SSNO^-$  was unstable at pH 7. Wedman *et al.* also prepared crystalline  $SSNO^-$  as its bis(triphenylphosphine)iminium salt ( $PNP^+SSNO^-$ ) based on the procedure published by Seel and Wagner (42). After re-dissolving the solid material in organic solvents, the UV-Vis absorbance maxima of  $PNP^+SSNO^-$  in acetone and methanol were measured by them to be at 448 nm and 422 nm, respectively. They claimed that the molecule was highly unstable when the crystals were dissolved in aqueous solutions or water was added to

organic solutes of  $\text{PNP}^+\text{SSNO}^-$ . Therefore, they suggested that the 412 nm absorbance observed by Cortese-Krott et. al. „may only be attributed to the presence of the mixture of polysulfides/sulfur sols”, generated as byproducts during NO-sulfide interactions. We prepared the same crystals following Seel and Wagner’s procedure (see Methods); however, closer microscopic inspection and exploratory X-ray crystallography of the crystalline material suggested it was highly inhomogeneous, with at least three clearly distinguishable morphologies, colours and geometries (data not shown), indicative of different inclusion complexes. This had already been described in Seel’s original paper (35) and acknowledged by Wedmann et al (42). Dissolution of this solid material in aqueous buffers resulted in the transient appearance of a 412 nm peak, followed by fast precipitation of a white solid (most likely colloidal sulfur), as observed when  $\text{SSNO}^-$ /sulfide mixtures are acidified. However, when the crystals were first dissolved in DMSO followed by drop-wise addition of an aqueous phosphate buffer pH 7 containing 1 mM sulfide in addition, the characteristic 412 nm feature exhibited much greater stability with  $\sim 20\%$  decomposition over 5 minutes (Figure 1).

Curiously, Wedmann et al also observed the appearance of a 420 nm peak with comparable stability when their crystals were dissolved in 300 mM phosphate buffer containing 1 mM sulfide (Figure 7E in ref (42)). However, they claimed that this could not possibly be due to  $\text{SSNO}^-$  because the latter would rapidly react with sulfide to give  $\text{HSNO}$ ; they concluded that it must therefore be due to inorganic polysulfides/sulfur sols. In order to shed further light onto this apparent paradox, we repeated their experiments using a different  $\text{SSNO}^-$  preparation and reversing the order of solvent alterations.  $\text{SSNO}^-$  (the 412 species) was prepared by the reaction of SNAP with excess sulfide in Tris/HCl buffer, as described before (9,11), and the aqueous mixture was then diluted 10-fold in methanol or acetone to investigate how its UV-Vis spectra in organic solvents compare to those measured after dissolving the  $\text{PNP}^+\text{SSNO}^-$  salt in similar solvents. Increasing the proportion of the organic solvent over water resulted in a bathochromic shift of the 412 nm feature, as described by Seel and some of us earlier (9,35). In a mixture of 90% acetone/10% Tris buffer the absorbance maximum shifted to 439 nm and in 90% MeOH/10% Tris buffer it was at 426 nm (Figure 2), very close to the ones observed by

Wedmann et al, Seel et al and us for the  $\text{PNP}^+\text{SSNO}^-$  salt. The close association between the observed absorbance maxima for the two distinct procedures/preparations, which apparently correlate very well with theoretically calculated solvatochromic effects using TD-DFT and QM/MM MD simulations (27), corroborate the notion that the observed characteristic UV-Vis bands in different solvents can both be attributed to  $\text{SSNO}^-$ .

As alluded to above, Filipovic et al proposed that the 412 nm peak in the SNAP/sulfide reaction mixture was potentially due to inorganic polysulfides/sulfur sols since they could be reduced by DTT (Figure 7J in ref (42)). However, we demonstrated in our previous study that in contrast to polysulfides, the 412 nm species generated during the reaction of nitrosothiols with sulfide is fully resistant towards DTT and cyanide (see Fig S5 in ref (11)). In fact, in order to eliminate the inorganic polysulfide species (which are formed as byproducts in the reaction of nitrosothiols with sulfide) from  $\text{SSNO}^-$  solutions, we here utilized this unique chemical property of the '412 species' the following way:  $\text{SSNO}^-$  solutions were prepared by the reaction of 3 mM SNAP and 30 mM sulfide. This reaction mixture contains inorganic polysulfides (11), accounting for ~50% of the initial SNAP concentration. Therefore, immediately after formation of the 412 nm peak the reaction mixture was passed through a Pierce Immobilized Reductant Column, containing beaded resin with immobilized sulfhydryl groups in order to selectively minimise the polysulfide content in that preparation. The solution was then bubbled with  $\text{N}_2$  for 5 min to eliminate the majority of reduced sulfide in the form of  $\text{H}_2\text{S}$  from the mixture. Using this procedure, the "cleaned-up"  $\text{SSNO}^-$  solutions contained < 20% of the initially generated polysulfides.<sup>1</sup>

In order to also obtain kinetic evidence that the 412 nm species in aqueous buffer is responsible for the UV-Vis absorbance maximum at 439 nm measured in 90% acetone/10% aqueous buffer, this "cleaned-up" aqueous  $\text{SSNO}^-$  solution was allowed to decompose on ice in the dark (the experiment was carried out on ice because in the absence of sulfide to stabilize  $\text{SSNO}^-$  it is considerably less stable, see below). Aliquots from this mixture were taken at distinct time points (at 20 min intervals), and a 10-fold

---

<sup>1</sup> Note that the polysulfide content is expected to be much less than 20%, because in the cold cyanolysis based measurements of residual polysulfides,  $\text{SSNO}^-$  decomposition also released substantial amounts of polysulfides during the necessary, relatively long incubation time with cyanide.



dilution was performed either in 200 mM pH 8.00 Tris/HCl buffer or acetone. The recorded time-dependent decrease in the absorbance values of the 412 nm peak, which was measured after dilution with buffer and that of the 439 nm peak, which was measured after dilution with acetone (i.e. in 90% acetone/10% aqueous buffer) were consistent with each other (see Fig. 3). Using the previously estimated  $\epsilon_{412} = 6000 \text{ M}^{-1}\text{cm}^{-1}$  the extinction coefficient at 439 nm in 90% acetone/10% aqueous buffer ( $\epsilon_{439} = 4340 \pm 202 \text{ M}^{-1}\text{cm}^{-1}$ ) was calculated as the average of the values that were measured at different time points. In light of the observed inhomogeneity of the crystalline material this is reasonably close to the one originally reported by Seel et al. at 448 nm ( $\epsilon_{448} = 2800 \text{ M}^{-1}\text{cm}^{-1}$ ).

In addition, we followed the decomposition of  $\text{SSNO}^-$  at increasing concentrations of sulfide and GSH, at distinct concentrations of  $\text{SSNO}^-$  and in solvents of different composition. The observed kinetic traces indicated that the reactions cannot be described by simple first order rate equations and a detailed mechanistic study with product analyses would be required to obtain deeper mechanistic insight into the decomposition process of  $\text{SSNO}^-$ . While this was beyond the aim of the current study, a number of conclusions can nevertheless be drawn from these analyses:

- 1) The kinetic traces depicted in Fig 4A and the measured half-lives of  $\text{SSNO}^-$  decomposition from the data shown in Fig 4B demonstrated that sulfide concentrations up to ~20 mM have a considerable stabilizing effect on  $\text{SSNO}^-$  under the applied experimental conditions. Due to the fact that complete elimination of sulfide from the aqueous buffer solutions of  $\text{SSNO}^-$  (where it is generated in the reactions of nitrosothiols with excess sulfide) is not possible, it is likely that the results shown in Figs 4A&B reflect conservative estimates of sulfide's true stabilizing effects. This could also partially account for the faster decomposition of  $\text{PNP}^+\text{SSNO}^-$  when the (inhomogeneous) crystalline material is dissolved in aqueous buffer systems, which contain no sulfide. In addition, Fig 4C&D show that at a similar concentration range, also GSH stabilizes  $\text{SSNO}^-$ . These observations, together with the fact that reactions of nitrosothiols with sulfide provide a mixture of reactive sulfur and nitrogen species (11), would suggest that the stabilizing effect of thiol compounds might possibly be due to capturing additional reactive species that facilitate  $\text{SSNO}^-$  decomposition. An alternative

explanation is that this effect is due to transition metal complexation, which has been demonstrated to contribute to the stabilizing effect of cysteine and other thiols towards S-nitrosothiols (17,44). However, this effect is unlikely based on the observed similarities in the kinetics of  $SSNO^-$  decomposition in the presence and absence of 200  $\mu M$  of the metal chelator diethylenetriamine pentaacetic acid (DTPA) at both 0 or 10 mM added sulfide (Fig 4B).

- 2) The results depicted in Figs 4A-D clearly indicate that in aqueous buffer systems at thiol concentrations up to  $\sim 40$  mM (thus well above the physiological range), the presence of either sulfide or GSH failed to accelerate the rate of  $SSNO^-$  decomposition. However, at concentrations  $>40$  mM both thiols started to shorten the half-life of  $SSNO^-$ , which may represent the emerging contribution of a bimolecular reaction between  $SSNO^-$  and the added thiol to the kinetics of  $SSNO^-$  decay. It should be noted that not fully eliminated polysulfides could have an effect on equilibrium (4) by shifting it to the right. However, if the bimolecular reaction between  $SSNO^-$  and sulfide would be a major driving force of  $SSNO^-$  decay, this phenomenon would only influence the decay kinetics by providing an intercept for a linear  $k_{obs}$  (obtained from the exponential fits of the kinetic traces) vs sulfide concentration plot. Based on these observations, at physiologically relevant concentrations of thiols in aqueous systems we propose that a bimolecular sulfur-transfer reaction between sulfide or GSH with  $SSNO^-$  can be excluded from mechanistic considerations regarding the fate of  $SSNO^-$ .
- 3) The decomposition kinetics of  $SSNO^-$  is independent of the starting  $SSNO^-$  concentration (Fig 4E&F), suggesting that it is not a second order process. This is in contrast to the disproportionation/conproportionation-driven decomposition of inorganic polysulfide species.
- 4) Contrary to the observation by Filipovic et al that  $SSNO^-$  can be rapidly attacked by sulfides or other nucleophiles in pure aprotic solvents like acetone or tetrahydrofuran, (but not in mixtures with hydroxylic solvents, see. ref.27), the stability of  $SSNO^-$  in our systems did not change substantially by changing the composition of the solvent system from 100% buffer to 60 % buffer/ 40 % acetone in the presence and absence of 20 mM GSH (Fig 4G&H). These observations agree

with our previous assumption that the relatively lower stabilities of  $\text{PNP}^+\text{SSNO}^-$  when it was dissolved in aqueous buffer systems or aprotic/protic solvent mixtures in the absence of sulfide were likely related to the inhomogeneity of the crystalline material (see above) and not to its self-decomposition and/or fast reactivity with sulfide or other thiols. To unambiguously reconcile these contradicting observations in mixed solvent systems, the preparation of a water-soluble perthionitrite-salt will be necessary, which will allow to determine the contributions of inhomogeneity and solvent effects on the stability of  $\text{SSNO}^-$ .

Thus, in refuting the claims by Wedmann et al., we conclude that the observed 412 peak is not due to inorganic polysulfides/sulfur sol because i) it cannot be reduced by DTT, sulfide, glutathione or cyanide, ii) its decomposition kinetics are independent of the starting concentration, and ii) in solutions in which preformed polysulfides as well as the residual sulfide was eliminated by immobilized -SH reductant and  $\text{N}_2$  bubbling, respectively, similar absorbance spectra were observed. Moreover, monitoring the decomposition of the 412 species by time-resolved UV-vis spectrophotometry revealed that it has similar spectral characteristics to that of the previously reported  $\text{PNP}^+\text{SSNO}^-$  salt, with absorbance maxima at 448 nm and 426 nm in acetone and methanol, respectively. Based on all these observations we argue that a major reaction product of SNAP and sulfide is indeed  $\text{SSNO}^-$ , that its lifetime is relatively long at pH 7 and that it cannot be reduced by thiols.

*SSNO<sup>-</sup> is also resistant towards the NADPH-driven cellular reducing systems*

Motivated by the surprising observation that thiol compounds (DTT, cysteine or GSH) are unable to reduce  $\text{SSNO}^-$  (11) we sought to investigate whether it might also escape the reducing power of the major NADPH-dependent cellular enzymatic machineries, i.e. the thioredoxin and the glutathione reductase systems. We previously demonstrated that *thioredoxin reductase 1* (TrxR1) can use NADPH to reduce inorganic and protein per/polysulfides, in reactions that were further accelerated upon the addition of the TrxR1 substrate *thioredoxin related protein of 14 kDa* (TRP14) (15). This observation was further corroborated here by following the enzymatic reactions using mass spectrometry based detection of inorganic polysulfide species (See Figure S1).

Furthermore, we recently obtained evidence in cells and *in vivo* that even the oxidized forms of protein per/polysulfides are substrates of the thioredoxin family of enzymes in a protein specific manner (14). In addition, *glutathione reductase* (GR) can use GSH and NADPH to catalytically reduce inorganic as well as protein per/polysulfides, in reactions that gain further catalytic power in the presence of *glutaredoxin* (Grx) (15). In light of these recent advances it was particularly interesting to find that upon the addition of physiologically relevant concentrations of the Trx and GR systems in different enzyme compositions we were unable to detect any effect on the slow “spontaneous” decomposition kinetics of SSNO<sup>-</sup> (Figure 4). Initially SSNO<sup>-</sup> was prepared by the reaction of 1 mM SNAP with 10 mM sulfide. Selective reduction of preformed inorganic polysulfides and sulfide removal was achieved by 500 μM DTT and N<sub>2</sub> degassing, which was followed by sequential addition of the components of either the Trx or the GSH enzymatic systems (see Figure 5). Neither NADPH on its own nor in the presence of GSH or TrxR1 or GSH+GR or TrxR1+TRP14 affected the slow decomposition of SSNO<sup>-</sup> in 200 mM Tris/HCl+100 μM DTPA buffer at pH 7.40 and RT.

Thus to the best of our knowledge, SSNO<sup>-</sup> to date represents the only investigated sulfane sulfur carrying compound that is capable of escaping the reducing power of these extremely efficient enzymatic systems. Olabe et al estimated the pK<sub>a</sub> for HSSNO to be ~5 (27), which means that at physiological pH the majority of it would be deprotonated. This could contribute to the inherent insensitivity of this molecule towards thiol-mediated reduction by hindering the nucleophilic attack of thiolates and strengthening the S-N bond. This observation suggests that SSNO<sup>-</sup> might function as a sulfane sulfur trafficking molecule, generating polysulfides *in situ* upon its slow decomposition, while being resistant towards the intracellular NADPH-driven reducing machineries (basically working as a slow endogenous sulfane sulfur donor). Inorganic polysulfides were on the other hand reduced by the Trx system in the presence of SSNO<sup>-</sup>. Based on repeated (n = 5) quantification by cold cyanolysis and the methylene blue method (as in ref (11)) after the formation of SSNO<sup>-</sup> was completed upon mixing 1 mM SNAP and 10 mM sulfide the reaction mixture contained 560 ± 190 μM sulfane sulfur equivalents and 9 ± 3 mM sulfide besides 300 ± 25 μM SSNO<sup>-</sup>. Incubation of these mixtures with 200 nM TrxR1, 650 μM

NADPH  $\pm$  2  $\mu$ M TRP14 for 10 min at RT, protected from light, followed by degassing with N<sub>2</sub> for an additional 5 min at RT in the dark, reduced the sulfane sulfur equivalents to 253  $\pm$  93  $\mu$ M and the residual sulfide to 111  $\pm$  20  $\mu$ M. (Note that the enzymatic reduction was likely much more efficient because the residual sulfane sulfur equivalents also contain inorganic polysulfides that were eliminated from SSNO<sup>-</sup> during the incubation with cyanide in the cold cyanolysis measurements.)

These observations indicated that the Trx system was functional and that selective reduction of polysulfides can be achieved while preserving the integrity of SSNO<sup>-</sup>. This selective reactivity of the Trx system also has methodological implications because it indicated that it can be used to enzymatically diminish inorganic polysulfide contents of freshly made SSNO<sup>-</sup> solutions, which can be followed by the elimination of the Trx family proteins using size exclusion chromatography (ultrafiltration) in order to avoid reduction of subsequent SSNO<sup>-</sup>-derived polysulfides (for more details see Materials and Methods).

*Inorganic polysulfides were identified as sulfane sulfur carrying products upon decomposition of SSNO<sup>-</sup>*

The formation of SSNO<sup>-</sup> in the reaction of nitrosothiols and sulfide is accompanied by auto-catalyzed formation of inorganic polysulfides. SSNO<sup>-</sup> appears to be sufficiently stable to be of physiological significance, but slowly decomposes to generate sulfane sulfur species. In our previous study we used cold cyanolysis and chloroform extraction-based methods to show that stoichiometric amounts of sulfane sulfur equivalents are released upon the decay of SSNO<sup>-</sup> (11). However, the chemical nature of these slowly generated sulfane sulfur species has not been investigated. Here we used LC-MS/MS to identify what inorganic polysulfides are generated in this system. Following the preparation of SSNO<sup>-</sup> by the reaction of SNAP with excess sulfide and enzymatic purification with 2 mM NADPH and 200 nM TrxR1, reaction mixtures were incubated at room temperature in the dark for 2 hours. 25  $\mu$ l aliquots of these mixtures were subjected to LC-MS/MS analyses after alkylation with 25 mM HPE-IAM (final concentration, 30 min, RT). Inorganic polysulfides were detected by selected reaction monitoring (as in ref (6), for SRM parameters see Supporting Information) with chain lengths up to 7 sulfurs (see S1-S7 chromatograms in

Figure 6). In this context, we caution that the actual speciation of the different chain length inorganic polysulfides shown in Figure 6 may differ substantially from that in real biological systems, due to the sensitivity of their distribution to the composition of the chemical environment as well as the experimental parameters used for detection. For example, we demonstrated that the nature and concentration of the alkylating agent that is used for their stabilization as well as the time of alkylation can substantially perturb polysulfide speciation equilibria (6). Thus, while the results of the experiment depicted in Figure 6 provides therefore qualitative information only it unequivocally demonstrates that inorganic polysulfides are eventual products of the SNAP-sulfide interaction and  $SSNO^-$  decomposition. In order to obtain quantitative data on how much of the sulfane sulfur equivalents can be accounted for as inorganic polysulfides upon the formation and decomposition of  $SSNO^-$ , isotopically labelled derivatives of all polysulfide species would have to be prepared, independently quantified and used as internal standards, which was well beyond the scope of the present study.

#### *SSNO<sup>-</sup> decomposition products induce slow and sustained polysulfidation of reduced glutathione (GSH)*

To experimentally address whether  $SSNO^-$  indeed induces polysulfidation of cysteine residues, we first investigated this using reduced glutathione (GSH).  $SSNO^-$  working solutions were prepared immediately before start of the kinetic experiments by the following procedure:  $SSNO^-$  was generated by reacting 1 mM SNAP with 10 mM  $Na_2S$  in 200 mM Tris/HCl+100  $\mu$ M DTPA buffer at pH 7.40. As stated above, besides  $SSNO^-$  (~300  $\mu$ M) the reaction mixture also contained ~500  $\mu$ M sulfane sulfur equivalents and ~9 mM sulfide. In order to eliminate the majority of the polysulfide content from this  $SSNO^-$  stock, we utilized the polysulfide-selective reducing potential of NADPH/TrxR1 (for experimental details see the Materials and Methods and “*SSNO<sup>-</sup> is also resistant towards the NADPH-driven cellular reducing systems*” sections). A control solution containing similar amounts of total polysulfides and sulfide (made by mixing freshly made  $Na_2S_2$  in water and sulfide solutions in 200 mM Tris/HCl, 100  $\mu$ M DTPA buffer at pH 7.40) was subjected to the same enzymatic reduction. TrxR1 was removed from the “cleaned-up”  $SSNO^-$  working solutions and from the controls by ultrafiltration. The reactions were

started by mixing these solutions (final concentration of  $\text{SSNO}^-$  was  $87 \pm 16 \mu\text{M}$ ) or controls (using a similar dilution factor as for the  $\text{SSNO}^-$  working solutions) with 1 mM GSH in 200 mM Tris/HCl+100  $\mu\text{M}$  DTPA buffer at  $\text{pH} = 7.40$  (the mixing time was considered as the 0 min time point of the kinetic runs); reactions were let to proceed at RT in the dark. At 0, 30, 60 and 120 minutes, 50  $\mu\text{l}$  aliquots were sampled from the incubation mixtures, and the reactions quenched by alkylation with 100 mM IAM (allowing for a minimum of 30 min alkylation at RT). Time-resolved formation and decomposition of the alkylated  $\text{GS(S)}_n\text{-IAM}$  ( $n=1-7$ ) species were detected by LC-MS/MS analysis. As shown in Figure 7, the reactions with  $\text{SSNO}^-$  induced significantly more glutathione per- and polysulfidation than the control samples at all time points (polysulfide formation in the controls, in particular the short-chain derivatives, was likely due to incomplete elimination of polysulfur species). An interesting observation in this system was the fact that the concentrations of longer-chain glutathione polysulfides (S6 and S7) steadily increased in the  $\text{SSNO}^-$  incubated with GSH, a behavior not observed in the controls. While polysulfide speciation may not reflect the true distribution of these products in the incubate (as discussed previously (6)), these experiments nevertheless demonstrate a sustained polysulfidation potential of  $\text{SSNO}^-$  using a biologically relevant thiol target (GSH) over a timescale similar to that of its decomposition. This observation together with the fact that under these conditions a direct reaction between  $\text{SSNO}^-$  and GSH was excluded on kinetic grounds (see Fig 4 C&D) suggest that the time resolved per/polysulfidation of GSH shown in Fig 7 was induced by  $\text{SSNO}^-$  released inorganic polysulfides.

#### *SSNO<sup>-</sup> decomposition products can induce sustained polysulfidation of thiol proteins*

Next,  $\text{SSNO}^-$  induced persulfidation was studied using the protein model, human serum albumin. We previously demonstrated that the free sulfhydryl group of the only cysteine residue that is not engaged in intramolecular structural disulfide bonds, Cys34, is prone to polysulfidation by inorganic polysulfides, which can be detected by our ProPerDP method (15). This system can therefore be used to study the potential polysulfidating effects of  $\text{SSNO}^-$  or its decomposition products on protein thiol targets. To this end,  $\text{SSNO}^-$  and control mixtures were prepared and purified from preformed polysulfides as described for the GSH experiments above, before reaction with HSA (containing reduced Cys34, see

Methods) at RT, protected from light to give a reaction mixture of  $48 \pm 9 \mu\text{M}$   $\text{SSNO}^-$  (or control solution at a similar dilution factor) with  $7.5 \mu\text{M}$  HSA. Aliquots from each reaction mixture were taken at 0, 20, 40 and 60 minutes, followed by the ProPerDP assay to detect protein persulfide formation (13). The persulfidated fraction of HSA was detected following separation on non-reducing 12% polyacrylamide gels, followed by western blotting and visualization as described in ref (15) (for the detailed protocol, please visit Materials and Methods section). As shown in Figure 8, increasing amounts of HSA-SSH were detected on a similar timescale as  $\text{SSNO}^-$  is expected to decompose under these conditions. No HSA-SSH was detected in the control samples, suggesting that the selective abolishment of in situ generated inorganic polysulfide byproducts by the NADPH-TrxR1 system was effective. (Note that this method is less sensitive compared to the mass spectrometry-based detection of polysulfide species shown in Figure 6 and that HSA-polysulfidation by inorganic polysulfides represents a true equilibrium, where an excess of polysulfides is needed to fully polysulfidate Cys34 (15)). Figure 8 indicated that the kinetics of HSA-SSH generation upon  $\text{SSNO}^-$  treatment is indeed consistent with the kinetics of  $\text{SSNO}^-$  decay under these conditions, corroborating that the delayed persulfidating effects are caused by its decomposition products rather than  $\text{SSNO}^-$  itself (the concentration of which was highest at the beginning).

#### *SSNO<sup>-</sup> can induce sustained activation of TRPA1 ion channels*

We next investigated whether  $\text{SSNO}^-$ , the major product of NO and sulfide interaction, might also account for the previously observed cooperative action of NO and sulfide species on TRPA1 channel activity (16). In these experiments,  $\text{SSNO}^-$  was prepared using a different S-nitrosothiol precursor, GSNO in order to avoid the possible TRPA1 antagonistic effects of N-acetyl-DL- penicillamine generated as a byproduct of the SNAP/sulfide interaction (36).

The  $\text{SSNO}^-$  preparation generated from GSNO/sulfide was subjected to enzymatic reduction of concomitantly generated inorganic polysulfides, followed by  $\text{N}_2$  bubbling to remove the majority of the remaining sulfide (as for the other  $\text{SSNO}^-$  preparations and described in the Methods section).  $\text{SSNO}^-$  and a control sample (a solution of  $9 \text{ mM}$   $\text{Na}_2\text{S}$  +  $0.5 \text{ M}$   $\text{Na}_2\text{S}_2$ , which was subjected to the same treatment) were allowed to decompose at



RT in the dark. Aliquots from the incubated solutions were taken at 0, 30 and 60 and 120 minutes, diluted to a final concentration of 10  $\mu\text{M}$  SSNO<sup>-</sup> (using a similar dilution factor for the control samples) and added to TRPA1 expressing CHO cells previously stained with the Ca<sup>2+</sup> ion specific fluorescent dye Fluo-4. The intracellular fluorescence signal generated was immediately analyzed by flow cytometry. TRPA1 deficient cells were also treated and analyzed in the same manner, but they did not reveal any intracellular fluorescence above baseline upon any treatment, which corroborated that the detected Ca<sup>2+</sup> influx can indeed be attributed to the activation of TRPA1 ion channels in this cell line (Figure S2). A parallel batch of cells was reacted with the selective TRPA1 receptor agonist mustard-oil (100  $\mu\text{M}$  in ECS) as positive control. The obtained average fluorescence signal in these positive control samples was set as 100% and the fluorescence intensity in the presence of SSNO<sup>-</sup> or control solutions were expressed as % of this value.

Figure 9 shows, that treatment of cells with 10  $\mu\text{M}$  SSNO<sup>-</sup>, resulted in a constant TRPA1 activation over 2 hours corroborating that most likely due to the slow but continuous release of inorganic polysulfides, SSNO<sup>-</sup> can induce a sustained activation of these ion channels. On the contrary, a statistically significant ( $P = 0,0136$ ) decrease in Ca<sup>2+</sup> influx was detected in cells treated with the control solutions, which is in line with a transient activation of TRPA1 by the relatively unstable residual inorganic polysulfides (due to non-complete TrxR1-mediated reduction and/or remaining sulfide).

Taken together, our data suggest that SSNO<sup>-</sup> indeed plays a role in the cooperative actions of NO and sulfide on TRPA1 channel activation. In addition, our data agrees with the proposal by Kimura and coworkers that the immediate activation of TRPA1 channels by reaction mixtures of nitrosothiols and sulfide are likely due to preformed polysulfide species (31). However, preformed polysulfide species would only elicit a transient activation of TRPA1 channels, whereas SSNO<sup>-</sup> induces sustained TRPA1 activation by providing a slow flux of inorganic polysulfide species.

## Conclusions

In the present study we obtained corroborating evidence for the fact that  $SSNO^-$ , a major product of the chemical reactions between sulfide and NO species, is indeed relatively stable in aqueous solutions of physiological pH. Furthermore, we confirm that it is stabilized by the presence of excess sulfide and fully resistant towards reduction by thiols. Unexpectedly, we also find that  $SSNO^-$  escapes the reducing power of the NADPH-driven biological reduction machineries. We believe that these properties have important biological implications. To the best of our knowledge,  $SSNO^-$  is the first biologically relevant sulfane sulfur carrying molecule that cannot be effectively reduced by thiols or by the TrxR and/or GR systems. Furthermore, we here show that the slow decomposition of  $SSNO^-$  liberates inorganic polysulfides, which efficiently convert glutathione and protein Cys thiols into their corresponding per- and polysulfide derivatives. The potential biological implication of these reactions was demonstrated exemplary by the activation of TRPA1 channels. Specifically, we demonstrated that in contrast to the transient activation of these channels by polysulfides,  $SSNO^-$  induces long-term potentiation of TRPA1 channels by generating a slow *in situ* flux of inorganic polysulfides. Notwithstanding the use of simple *in vitro* model systems to demonstrate biological relevance, these properties of  $SSNO^-$  would seem to offer unique opportunities for cell signaling by enabling sulfur and nitrogen trafficking within the reducing environment of the cytosol, with targeted release of both NO and polysulfide equivalents.

## Innovation

Based on *in vitro* data we propose that  $SSNO^-$  is an important chemical entity in the crosstalk between NO and  $H_2S$ /persulfide signaling. It may act as a dual sulfane sulfur and NO trafficking molecule in biology, which can escape the cellular reducing power. By slowly releasing peptide/protein Cys-persulfidating inorganic polysulfide species and NO distant to its site of generation, this S/N hybrid species may act as a mobile carrier of sulfane sulfur equivalents and NO to trigger sustained intracellular effects.

## Materials and Methods

### *Reagents, SSNO<sup>-</sup> preparation*

Sodium disulfide (Na<sub>2</sub>S<sub>2</sub>) was kindly provided by Dojindo Laboratories (Munich, Germany and Kumamoto, Japan). Recombinant rat thioredoxin reductase 1 (TrxR1) and the thioredoxin-related protein of 14 kDa (TRP14) were kindly provided by Prof. Elias Arnér. Glutathione reductase (GR) was from Sigma-Aldrich. All other reagents were purchased at the highest purity available either from Sigma-Aldrich, Cayman Chemicals, VWR Chemicals, Santa Cruz Biotechnology or Thermo Fisher Scientific.

Sulfide stock solutions were prepared in water as previously described (33) and diluted further in the indicated buffer immediately before use. Although all precautions were undertaken to avoid the formation of oxidation products (including polysulfides) in these stock solutions, their presence (at least in trace amounts) cannot be prevented completely under aerobic conditions. Polysulfide stock solutions were prepared in either ultrapure water or in the indicated buffer by dissolving either technical potassium polysulfide (K<sub>2</sub>S<sub>x</sub>; a mixture of sulfide and polysulfides of different chain lengths), sodium disulfide (Na<sub>2</sub>S<sub>2</sub>), sodium trisulfide (Na<sub>2</sub>S<sub>3</sub>) or sodium tetrasulfide (Na<sub>2</sub>S<sub>4</sub>) salts. All solutions were prepared fresh immediately before use in experiments.

10 mM aqueous stock solutions of S-nitroso-N-acetyl-D,L-penicillamine (SNAP) or S-nitroso-L-glutathione (GSNO) were freshly prepared by dissolving crystalline material in 200 mM tris(hydroxymethyl)aminomethane (Tris) buffer, pH 7.4 and diluted further immediately before use or divided into aliquots and kept at -80 °C until use. Stock solutions of SSNO<sup>-</sup> were prepared by reacting 1 mM SNAP or GSNO with 10 mM Na<sub>2</sub>S in 200 mM Tris (pH 7.4).

Inorganic polysulfides are present in sulfide stock solutions as contaminants and produced *in situ* during SSNO<sup>-</sup> preparation or decomposition. Their selective reduction (where indicated) was carried out either using a Pierce<sup>TM</sup> Immobilized Reductant Column (supported with 6% crosslinked beaded agarose and activated by a thiol-based reducing agent to enable solid-phase reduction of peptide and protein disulfide bonds) based on the manufacturer's instructions (<https://assets.thermofisher.com/TFS->

[Assets/LSG/manuals/MAN0011211\\_Immobil\\_Reductant\\_Column\\_UG.pdf](#)) after

conditioning the column with 10 mM DTT or enzymatically using the NADPH–TrxR1 system as indicated at each experiment. Both SSNO<sup>-</sup> preparation and inorganic polysulfide reduction resulted in sulfide (H<sub>2</sub>S) accumulation, which was eliminated from the solution by degassing with N<sub>2</sub> for an additional 5 minutes, protected from light following the reduction. This „purified” SSNO<sup>-</sup> was then used for per- and polysulfidation studies, which were performed on reduced glutathione, human serum albumin and TRPA1 expressing Chinese hamster ovary (CHO) cells. Note that N<sub>2</sub> bubbling must have initially eliminated a large fraction of dissolved oxygen from these “purified” SSNO<sup>-</sup> solutions, but they were subsequently exposed to laboratory atmosphere and dissolved O<sub>2</sub> concentrations were not monitored throughout these experiments.

### *Chemical characterization of SSNO<sup>-</sup>*

#### *Uv-vis spectra of PNP<sup>+</sup>SSNO<sup>-</sup> in phosphate buffer in the presence of sulfide*

Preparation of crystalline bis(triphenylphosphine)iminium perthionitrite (PNP<sup>+</sup>SSNO<sup>-</sup>) was carried out in a three-step procedure following literature protocols (29,34,35). Briefly, first bis(triphenylphosphine)iminium chloride (PNP<sup>+</sup>Cl<sup>-</sup>) was made treating PPh<sub>3</sub> in 1,1,2,2-tetrachloroethane with one equivalent of chlorine gas at -20 °C and subsequent boiling of the resulting slurry in the presence of hydroxylamine hydrochloride (34). PNP<sup>+</sup>Cl<sup>-</sup> was isolated by adding the reaction mixture to ethyl acetate. Subsequent recrystallization from hot water afforded pure PNP<sup>+</sup>Cl<sup>-</sup> as a white crystalline solid. PNP<sup>+</sup>Cl<sup>-</sup> was then converted to the nitrite salt by treating its warm concentrated aqueous solution with saturated NaNO<sub>2</sub> solution (29). The solid formed was filtered, dried and recrystallized using Et<sub>2</sub>O/acetone. For the preparation of PNP<sup>+</sup>SSNO<sup>-</sup> the white needles of the nitrite salt (PNP<sup>+</sup>NO<sub>2</sub><sup>-</sup>; 2.5 g, 4.28 mmol) were reacted with elementary sulfur (S<sub>8</sub>; 0.274 g, 8.56 mmol) in pre-dried, freshly distilled and nitrogen-saturated acetone (70 ml) under an atmosphere of purified N<sub>2</sub> using standard Schlenk techniques in the dark (35). After overnight reaction, the dark red reaction mixture was filtered under N<sub>2</sub> and chilled to -78 °C. Carefully, absolute Et<sub>2</sub>O (stored over sodium and saturated with N<sub>2</sub> prior to use) was layered on top of the filtrate in a Schlenk vial and left to warm up to RT in the dark.

After 3 days the mother liquor was decanted under  $N_2$  from the orange-red crystalline solid formed. The solid was rinsed with 3 portions of dry  $Et_2O$  (3-4 ml) and dried under vacuum (yield: 0.487 g, 18 %). UV-Vis spectra were recorded using a Perkin Elmer Lambda 2S UV/VIS spectrophotometer using quartz cuvettes with 1 cm path lengths.

#### *Uv-vis spectra of the reaction products of SNAP and sulfide in solvent mixtures*

$SSNO^-$  stock solutions were prepared by reacting 3 mM SNAP with 30 mM  $Na_2S$  in 200 mM Tris/HCl (pH 7.4) (9). Following the selective reduction of *in situ* generated polysulfides by a reductant column (see above) activated by 10 mM DTT and sulfide removal by degassing with  $N_2$  for an additional 5 min at RT. The  $SSNO^-$  stock solution was allowed to decompose at RT, protected from light. Aliquots from this incubation solution were taken at 0, 20, 40 and 60 min and 10x dilutions were performed at each time point both in 200 mM Tris/HCl (pH 7.4) and acetone. UV/Vis spectra of these diluted solutions were taken using an Agilent Cary 8454 diode-array spectrophotometer with quartz cuvettes of 1.00 cm path length, and concentrations of  $SSNO^-$  at each time point were calculated using the measured absorbance and previously determined  $\epsilon$  values (which were found to be  $6000 M^{-1}cm^{-1}$  in aqueous media). The  $\epsilon = 4340 \pm 202 M^{-1}cm^{-1}$  value for  $SSNO^-$  in 90% acetone 10% 200 mM Tris (pH 7.4) was calculated from the obtained spectra at 439 nm by using the calculated concentrations of the decomposing  $SSNO^-$  solution at different time points in buffered media before dilution with acetone.

#### *Effects of $H_2S$ , glutathione, $SSNO^-$ concentrations and solvent composition on the decomposition kinetics of $SSNO^-$*

$SSNO^-$  stock solutions were prepared by mixing 6 mM SNAP with 60 mM  $Na_2S$  in 100 mM Tris/HCl (pH 7.4). This was followed by the reduction of *in situ* generated polysulfides by 100 nM TrxR1 and 1 mM NADPH for 15 minutes at RT and sulfide removal by degassing with  $N_2$  for an additional 10 min. Concentration of  $SSNO^-$  stock solution was calculated using measured absorbance at 412 nm and previously determined  $\epsilon$  value of  $6000 M^{-1} cm^{-1}$  in aqueous media (11).

22

Na<sub>2</sub>S solutions were prepared as described above and mixed with SSNO<sup>-</sup> in 1:1 ratio immediately before measurement. DTPA (when added in Fig 4B) was introduced to the reaction mixtures at this time point.

GSH stock solutions were prepared by dissolving crystalline material in 200 mM Tris/HCl (pH 7.40). The pH of GSH stock solutions were set to 7.4 before further dilution with buffer or buffer/acetone mixtures. GSH in buffer solutions were mixed with SSNO<sup>-</sup> in 1:1 ratio immediately before measurement and acetone containing solutions with or without GSH were added to SSNO<sup>-</sup> immediately before measurement in a 1:1 ratio.

Decomposition of SSNO<sup>-</sup> was followed at 412 nm using Tecan Spark 10M plate reader in 96 well microplate format.

#### *Studying the reduction of SSNO<sup>-</sup> towards the NADPH-driven cellular reducing systems*

To study the effects of the NADPH–TrxR1–Trx/TRP14 or NADPH–GR–GSH enzymatic systems on the decomposition of SSNO<sup>-</sup>, an aqueous mixture of 1 mM SNAP and 10 mM sulfide was prepared in 200 mM Tris/HCl buffer, pH = 7.40. Selective removal of in situ generated inorganic polysulfides was achieved by reacting this mixture with 500 μM DTT at +4 °C, protected from light for 15 minutes, then the solution was degassed with N<sub>2</sub> at +4 °C, protected from light for an additional 15 minutes, in order to eliminate sulfide excess. After polysulfide and sulfide removal, 250 μl of this solution was pipetted into wells, and then each components of the enzymatic system were separately added to the solution. All kinetic experiments were carried out in Tris buffer (200 mM Tris/HCl and 100 μM DTPA, pH 7.40) at RT, in 96-well microtiter plates using a BioTek Powerwave XS plate reader. The presence of the enzyme systems on the decomposition of SSNO<sup>-</sup> was studied by following the absorbance changes at 412 nm, which is the λ<sub>max</sub> of SSNO<sup>-</sup>. Timescale and concentration conditions were optimized according to preliminary experiments by monitoring the reaction at 340 nm which is the λ<sub>max</sub> of NADPH. The pathlength correction mode of the plate reader was used in order to record proper absorbance values (l=1 cm) for further calculations.

## *LC/MS measurements of inorganic polysulfides*

### *Enzymatic reduction of inorganic polysulfides*

To study timescale and efficiency of the enzymatic reduction of inorganic polysulfides, 100  $\mu\text{M}$   $\text{Na}_2\text{S}_2$  was incubated with 250  $\mu\text{M}$  NADPH and 100 nM TrxR1, or 250  $\mu\text{M}$  NADPH, 100 nM TrxR1 and 2  $\mu\text{M}$  TRP14 at RT, protected from light. 25  $\mu\text{l}$  of these reaction mixtures were taken at 0, 5, 10, 15, 30 and 60 min and incubated with 25  $\mu\text{l}$  of 50 mM HPE – IAM at RT for 30 min. Then, 5  $\mu\text{l}$  of 50% TCA was added to the samples, followed by vigorous vortexing and centrifuging at 3000 g for 5 min. Samples were subjected to LC/MS analysis and the corresponding S1-S7 – HPE-IAM adducts were detected. The system consisted of a Thermo Ultimate 3000 HPLC equipped with binary pump, cooled autosampler and UV/Vis detector connected to a Thermo LTQ-XL linear ion trap mass spectrometer. After HPE-IAM labeling, 20  $\mu\text{l}$  of the acidified samples were injected on a Phenomenex Kinetex C18 2,6 $\mu\text{m}$  50x2.1 mm column for separation using eluents  $\text{H}_2\text{O}/0.1\%\text{FA}$  (A) and  $\text{MeOH}/0.1\%\text{FA}$  (B) and the following profile: Initial composition of 5% B was increased linearly to 90% B in 15 minutes, followed by a 2 minute decrease to 5% B and a 3 minute equilibration before the next injection. MS/MS detection was used to quantify the species, unless stated otherwise, in which case only the parent ions were detected in single ion monitoring mode. In all cases an ESI ion source was used in positive mode employing a spray voltage of 4 KV, capillary voltage of 14 V and a capillary temperature of 300°C. The detected SRM parameters using CID at a normalized energy of 35 % are shown in Table 1, for SIM mode only the parent masses were selected without further CID fragmentation. Isolation windows for all selected ions were set to  $\pm 0.5$  m/z.

### *Detection of inorganic polysulfides upon the decomposition of SSNO<sup>-</sup>*

In order to study the formation of inorganic polysulfides during SSNO<sup>-</sup> decomposition, a mixture of 1 mM SNAP and 10 mM sulfide was prepared and enzymatic purification was performed by incubation with 2 mM NADPH and 200 nM TrxR1, protected from light. 25  $\mu\text{l}$  aliquots from this reaction mixture were taken at the indicated time points and reacted with 25  $\mu\text{l}$  of 50 mM HPE – IAM according to Materials and Methods

section. Protein removal was achieved by TCA precipitation, then samples were centrifuged and subjected to LC-MS/MS analysis as described above.

#### *SSNO<sup>-</sup>-induced Sustained polysulfidation on GSH*

To study the per- and polysulfidation effects of SSNO<sup>-</sup> on GSH, 1 mM reduced glutathione was incubated with enzymatically purified (10 minutes incubation with 200 nM TrxR1 + 2 mM NADPH, followed by 5 min degassing with N<sub>2</sub>) 87 ± 16 μM SSNO<sup>-</sup> at RT, protected from light. Aliquots were taken from the reaction mixture at 0, 30, 60 and 120 min and alkylated with 100 mM IAM for 30 min at RT. Samples were then subjected to UPLC–MS/MS analysis or kept at -25 °C until analysis. Separation was performed on a 1.6 μm diameter Modus 100 x 2.2 mm Aqua UPLC column (Chromatography Direct). Glutathione per/polysulfur species were detected by a Waters Xevo TQ–S triple quadrupole detector and identified in multiple reaction monitoring (MRM) mode as described previously (37). As a control, a solution containing 500 μM Na<sub>2</sub>S<sub>2</sub> and 9 mM Na<sub>2</sub>S was prepared, purified and reacted with 1 mM GSH in parallel with the SNAP–sulfide reaction mixture. Samples from this control reaction were taken similarly at 0, 30, 60 and 120 minutes, alkylated with 100 mM IAM for 30 min at RT and then subjected to UPLC–MS/MS analysis or kept at -25 °C until analysis.

#### *Time resolved formation of HSA-SSH upon SSNO<sup>-</sup> treatment*

The reduction of Cysteine-34 of human serum albumin (HSA) was achieved by incubation with 5 mM DTT in 200 mM Tris-HCl/100 μM DTPA buffer at pH 7.40, at +4 °C for at least 30 min (3). Excess DTT was removed by desalting with Zeba Desalting Spin Columns (0.5 ml, 7KMWCO). Protein quantification was performed by the Bradford assay, followed by the treatment of 0.5 mg/ml of pre-reduced HSA with enzymatically (10 minutes incubation with 650 μM NADPH and 200 nM TrxR1) purified SSNO<sup>-</sup> and control solutions. Aliquots were taken from the reaction mixtures at 0, 20, 40 and 60 min, samples were desalted using Zeba Desalting Spin Columns (0.5 ml, 7K MWCO) and human serum albumin persulfide (HSA-SSH) was detected by the Protein Persulfide Detection Protocol (ProPerDP) method (15). Briefly, desalted protein solutions were alkylated with 1 mM iodoacetyl-biotin (IAB) (1 hour at RT, protected from light). IAB excess was removed by gel filtration and by ultrafiltration using Amicon microconcentrators (using either AMICON ULTRA



0.5ML - 30KDa cutoff, Ultracel-30 regenerated cellulose membrane or 0.5 ml sample volume, Merck Millipore). Biotinylated proteins were pulled down by streptavidin-coated magnetic beads (Sigma) according to the following procedure: after incubation on a rocking platform at RT for 30 min, magnetic beads were separated from the solution with a magnetic particle separator (DynaL MPC-M). Then, supernatant was placed in a clean tube, and the beads were washed with Tris-buffered saline containing 0.05% Tween 20 (TBST) three times, in order to eliminate nonspecific adhesion. Beads were then resuspended and incubated with 5 mM tris(2-carboxyethyl)phosphine (TCEP) (30 min, RT) while shaking, followed by magnetic separation. Beads were finally boiled at 100°C for 3 min in sodium dodecyl sulfate polyacrylamide gel electrophoresis (SDS-PAGE) sample loading buffer to elute all bound material. The samples were then analyzed by SDS-PAGE gel electrophoresis followed by Western blot analyses (see below). Protein concentrations were monitored throughout the process by the Bradford assay (Bio-Rad) and adjusted to the same concentration of HSA in each sample.

#### *SDS-PAGE gel electrophoresis*

Equal amounts of total protein were incubated with the streptavidin-coated beads in the case of each given gel and blot. Samples containing ~50 ng protein were run on non-reducing 12% polyacrylamide gels at 120 V for at least 90 min. Gel bands were visualized following western blotting, followed by 5-bromo-4-chloro-3-indolyl phosphate–nitro blue tetrazolium (BCIP-NBT, Merck)) staining and imaged on Syngene G:Box gel documentation system.

#### *Western blotting against HSA*

Following SDS-PAGE gel electrophoresis, plasma samples were transferred to polyvinylidene difluoride membranes (130 V, 90 minutes), which were then blocked overnight in 3% bovine serum albumin (BSA) solution at 4°C. Membranes were subsequently incubated for 1 hour in anti-albumin antibody (SigmaA0433), diluted 1:10,000 in 3% BSA. Subsequently, the membranes were washed three times with TBST buffer and incubated for 1 hour in alkaline phosphatase–conjugated secondary antibody (Sigma A3687), diluted 1:10,000 in 3% BSA. Membranes were washed again three times in

Tris-buffered saline, 0.1% Tween 20 (TBST) buffer, and bands were visualized by BCIP–NBT staining. Quantitative analysis of the bands was performed by using the ImageJ software (NIH).

#### *Measurement of Ca<sup>2+</sup> influx in TRPA1-expressing CHO cells in response to SSNO<sup>-</sup> by flow cytometry*

TRPA1 expressing CHO cells were kindly provided by Prof. Zoltán Sándor and maintained in culture as described previously (5). For cell harvest, the culture medium (500 mL Dulbecco's-Modified Eagle Medium (DMEM), 50 mL fetal bovine serum albumin, 10 mL L-glutamine (200 mmol/L), 10 mL MEM non-essential amino acid solution, 500 µL penicillin and streptomycin) was gently removed from the cells and trypsin solution (250 µL, 0.1% in PBS) was applied for 5 min. For each sample, approximately 10<sup>4</sup> TRPA1-expressing CHO cells were resuspended in 100 µL cell culture medium. Cells were incubated with Fluo-4 AM (Invitrogen, 0.4 µL, 1 µg/µL in dimethylsulfoxide (DMSO)) for 30 min, at 37 °C. 400 µL of extracellular solution (ECS) was then added (400 µL, containing (in mmol/L): NaCl, 160; KCl, 2.5; CaCl<sub>2</sub>, 1; MgCl<sub>2</sub>, 2; HEPES, 10; glucose, 10; pH 7.3). to reach a final volume of 500 µL. Then, the appropriate volumes of SSNO<sup>-</sup> and control solutions were taken from the reaction mixtures, diluted to 500 µL in ECS to reach a final 10 µM concentration of SSNO<sup>-</sup>, added to the cell suspensions and analysed by flow cytometry immediately. Fluo-4 AM was excited by 488 nm laser; fluorescence was detected at 504 nm. Mean green fluorescence of the samples was compared to base fluorescence of dye-loaded control cells. As positive control, cell groups were reacted with the selective TRPA1 receptor agonist mustard-oil (100 µmol/L in ECS) and analysed by flow cytometry.

#### *Data analysis*

Plotting and statistical analysis were performed using Graphpad Prism 5.03 (Graphpad Software Inc.). Measured values were compared using Student's T-test. To determine tendencies, deviation of the slopes from zero from linear regression analysis were tested. Relevant significances are denoted on the graphs depending on the obtained P values in the following way: ≥0.05 = ns, 0.01 to 0.05 = \*, 0.001 to 0.01 = \*\*, ≤0.001 = \*\*\*.

## Acknowledgements

**Funding:** This work was supported by the 2019 Hungarian Thematic Excellence Program (TUDFO/51757/2019-ITM), by the Hungarian National Research, Development and Innovation Office under grants nr. KH\_126766 and K\_129286, by EFOP 3.6.1-16.2016.00004, EFOP-3.6.3-VEKOP-16-2017-00009, OTKA PD 112171 grants and by the ÚNKP-16-1 and ÚNKP-17-1 New National Excellence Program of the Ministry of Human Capacities. We thank the NIHR Southampton Center for Biomedical Research and the University of Southampton Medical School for support with the mass spectrometry experiments and Dr. Mateusz Pitak at the EPSRC National Crystallography Service & Southampton Diffraction Centre of the University of Southampton for assistance with X-ray diffraction studies of the different components of the  $[\text{PNP}^+\text{SSNO}^-]$  crystals.

We are indebted to Prof. Elias Arnér for providing the thioredoxin family proteins, Prof. Miriam Cortese-Krott for stimulating discussions in the early part of the project, and the unknown reviewers of this manuscript for their insightful criticism. Noémi Balog, Éva Sággy, Maya Payrits, Gábor Pozsgai and Éva Szőke are acknowledged for their supports to different aspects of the experimental work discussed above.

The authors declare that they have no conflict of interests.

### Author Disclosure Statement:

The authors declare no conflict of interest.

**List of abbreviations**

BCIP-NBT	5-bromo-4-chloro-3-indolyl phosphate–nitro blue tetrazolium
BSA	bovine serum albumin
CHO	Chinese hamster ovary
CO	carbon-monoxide
Cys	cysteine
DMEM	Dulbecco's-Modified Eagle Medium
DMSO	dimethylsulfoxide
DTPA	diethylenetriaminepentaacetic acid
DTT	dithiotreitol
ECS	extracellular solution
GR	glutathione reductase
Grx	glutaredoxin
GSH	reduced glutathione
GSNO	S-nitroso-L-glutathione
H <sub>2</sub> S	hydrogen sulfide
HAS-SSH	human serum albumin persulfide
HEPES	4-(2-hydroxyethyl)-1-piperazineethanesulfonic acid
HNO	nitroxyl
HPE-IAM	β-(4-hydroxyphenyl)ethyl iodoacetamide
HSA	human serum albumin

HSNO	thionitrous acid
IAB	iodoacetyl-biotin
IAM	iodoacetamide
$K_2S_x$	a mixture of sulfide and polysulfides of different chain lengths
MRM	multiple reaction monitoring
$Na_2S_2$	sodium disulfide
$Na_2S_3$	sodium trisulfide
$Na_2S_4$	sodium tetrasulfide
NADPH	nicotinamide-adenine dinucleotide phosphate
NO	nitric-oxide
PBS	phosphate buffered saline
$PNP^+Cl^-$	bis(triphenylphosphine)iminium chloride
$PNP^+SSNO^-$	bis(triphenylphosphine)iminium perthionitrite
ProPerDP	Protein Persulfide Detection Protocol
RSI	Reactive Species Interactome
RSNO	S-nitrosothiols
RT	room temperature
SDS-PAGE	sodium dodecyl sulfate polyacrylamide gel electrophoresis
SNAP	S-nitroso-N-acetyl-D,L-penicillamine
$SSNO^-$	nitrosopersulfide
SULFI/NO	dinitrososulfite

TBST	Tris-buffered saline, 0.1% Tween 20
TCA	trichloroacetic acid
TCEP	tris(2-carboxyethyl)phosphine
Tris	tris(hydroxymethyl)aminomethane
TRP14	thioredoxin-related protein of 14 kDa
TRPA1	transient receptor potential ankyrin 1
TrxR	thioredoxin reductase
TrxR1	thioredoxin reductase 1
UV-Visible	UV-Vis

## References

1. Abe K, Kimura H. The possible role of hydrogen sulfide as an endogenous neuromodulator. *J Neurosci* 16: 1066-1071, 1996.
2. Akaike T, Ida T, Wei FY, Nishida M, Kumagai Y, Alam MM, Ihara H, Sawa T, Matsunaga T, Kasamatsu S, Nishimura A, Morita M, Tomizawa K, Nishimura A, Watanabe S, Inaba K, Shima H, Tanuma N, Jung M, Fujii S, Watanabe Y, Ohmuraya M, Nagy P, Feelisch M, Fukuto JM, Motohashi H. Cysteinyl-tRNA synthetase governs cysteine polysulfidation and mitochondrial bioenergetics. *Nat Commun* 8: 1177, 2017.
3. Alvarez B, Carballal S, Turell L, Radi R. Formation and reactions of sulfenic acid in human serum albumin. *Methods Enzymol* 473: 117-36, 2010.
4. Bailey TS, Henthorn HA, Pluth MD. The Intersection of NO and H<sub>2</sub>S: Persulfides Generate NO from Nitrite through Polysulfide Formation. *Inorg Chem* 55: 12618-12625, 2016.
5. Bogdandi V. Biologically relevant mechanisms of cysteine polysulfidation. *PhD thesis*, 2019.
6. Bogdandi V, Ida T, Sutton TR, Bianco C, Ditroi T, Koster G, Henthorn HA, Minnion M, Toscano JP, van der Vliet A, Pluth MD, Feelisch M, Fukuto JM, Akaike T, Nagy P. Speciation of reactive sulfur species and their reactions with alkylating agents: do we have any clue about what is present inside the cell? *Br J Pharmacol* 176: 646-670, 2019.
7. Cortese-Krott MM, Butler AR, Woollins JD, Feelisch M. Inorganic sulfur-nitrogen compounds: from gunpowder chemistry to the forefront of biological signaling. *Dalton Trans* 45: 5908-19, 2016.
8. Cortese-Krott MM, Fernandez BO, Kelm M, Butler AR, Feelisch M. On the chemical biology of the nitrite/sulfide interaction. *Nitric Oxide* 46: 14-24, 2015.
9. Cortese-Krott MM, Fernandez BO, Santos JL, Mergia E, Grman M, Nagy P, Kelm M, Butler A, Feelisch M. Nitrosopersulfide (SSNO(-)) accounts for sustained NO bioactivity of S-nitrosothiols following reaction with sulfide. *Redox Biol* 2: 234-44, 2014.

10. Cortese-Krott MM, Koning A, Kuhnle GGC, Nagy P, Bianco CL, Pasch A, Wink DA, Fukuto JM, Jackson AA, van Goor H, Olson KR, Feelisch M. The Reactive Species Interactome: Evolutionary Emergence, Biological Significance, and Opportunities for Redox Metabolomics and Personalized Medicine. *Antioxid Redox Signal* 27: 684-712, 2017.
11. Cortese-Krott MM, Kuhnle GGC, Dyson A, Fernandez BO, Grman M, DuMond JF, Barrow MP, McLeod G, Nakagawa H, Ondrias K, Nagy P, King SB, Saavedra J, Keefer L, Singer M, Kelm M, Butler AR, Feelisch M. The key bioactive reaction products of the NO/H<sub>2</sub>S interaction are S/N hybrid species, polysulfides, and nitroxyl. *Proc Natl Acad Sci U S A* 112: E4651-60, 2015.
12. Cortese-Krott MM, Santolini J, Wootton SA, Jackson AA, Feelisch M. Chapter 4 - The reactive species interactome. In: *Oxidative Stress*. edited by Sies H. Academic Press; 2020. pp. 51-64.
13. Doka E, Arner ESJ, Schmidt EE, Nagy P. ProPerDP: A Protein Persulfide Detection Protocol. *Methods Mol Biol* 2007: 51-77, 2019.
14. Doka E, Ida T, Dagnell M, Abiko Y, Luong NC, Balog N, Takata T, Espinosa B, Nishimura A, Cheng Q, Funato Y, Miki H, Fukuto JM, Prigge JR, Schmidt EE, Arner ESJ, Kumagai Y, Akaike T, Nagy P. Control of protein function through oxidation and reduction of persulfidated states. *Sci Adv* 6: eaax8358, 2020.
15. Doka E, Pader I, Biro A, Johansson K, Cheng Q, Ballago K, Prigge JR, Pastor-Flores D, Dick TP, Schmidt EE, Arner ES, Nagy P. A novel persulfide detection method reveals protein persulfide- and polysulfide-reducing functions of thioredoxin and glutathione systems. *Sci Adv* 2: e1500968, 2016.
16. Eberhardt M, Dux M, Namer B, Miljkovic J, Cordasic N, Will C, Kichko TI, de la Roche J, Fischer M, Suarez SA, Bikiel D, Dorsch K, Leffler A, Babes A, Lampert A, Lennerz JK, Jacobi J, Marti MA, Doctorovich F, Hogestatt ED, Zygmunt PM, Ivanovic-Burmazovic I, Messlinger K, Reeh P, Filipovic MR. H<sub>2</sub>S and NO cooperatively regulate vascular tone by activating a neuroendocrine HNO-TRPA1-CGRP signalling pathway. *Nat Commun* 5: 4381, 2014.
17. Feelisch M, te Poel M, Zamora R, Deussen A, Moncada S. Understanding the controversy over the identity of EDRF. *Nature* 368: 62-5, 1994.



18. Filipovic MR, Miljkovic J, Nauser T, Royzen M, Klos K, Shubina T, Koppenol WH, Lippard SJ, Ivanovic-Burmazovic I. Chemical characterization of the smallest S-nitrosothiol, HSNO; cellular cross-talk of H<sub>2</sub>S and S-nitrosothiols. *J Am Chem Soc* 134: 12016-27, 2012.
19. Gao XH, Krokowski D, Guan BJ, Bederman I, Majumder M, Parisien M, Diatchenko L, Kabil O, Willard B, Banerjee R, Wang B, Bebek G, Evans CR, Fox PL, Gerson SL, Hoppel CL, Liu M, Arvan P, Hatzoglou M. Quantitative H<sub>2</sub>S-mediated protein sulfhydration reveals metabolic reprogramming during the integrated stress response. *Elife* 4: e10067, 2015.
20. Hosoki R, Matsuki N, Kimura H. The possible role of hydrogen sulfide as an endogenous smooth muscle relaxant in synergy with nitric oxide. *Biochem Biophys Res Commun* 237: 527-531, 1997.
21. Ida T, Sawa T, Ihara H, Tsuchiya Y, Watanabe Y, Kumagai Y, Suematsu M, Motohashi H, Fujii S, Matsunaga T, Yamamoto M, Ono K, Devarie-Baez NO, Xian M, Fukuto JM, Akaike T. Reactive cysteine persulfides and S-polythiolation regulate oxidative stress and redox signaling. *Proc Natl Acad Sci U S A* 111: 7606-7611, 2014.
22. Ivanovic-Burmazovic I, Filipovic MR. Saying NO to H<sub>2</sub>S: A Story of HNO, HSNO, and SSNO(). *Inorg Chem* 58: 4039-4051, 2019.
23. Kevil C, Cortese-Krott MM, Nagy P, Papapetropoulos A, Feelisch M, Szabo C. Chapter 5 - Cooperative Interactions Between NO and H<sub>2</sub>S: Chemistry, Biology, Physiology, Pathophysiology. In: *Nitric Oxide (Third Edition)*. edited by Ignarro LJ, Freeman BA. Academic Press; 2017. pp. 57-83.
24. Kimura Y, Mikami Y, Osumi K, Tsugane M, Oka J, Kimura H. Polysulfides are possible H<sub>2</sub>S-derived signaling molecules in rat brain. *FASEB J* 27: 2451-7, 2013.
25. Kimura Y, Toyofuku Y, Koike S, Shibuya N, Nagahara N, Lefer D, Ogasawara Y, Kimura H. Identification of H<sub>2</sub>S<sub>3</sub> and H<sub>2</sub>S produced by 3-mercaptopyruvate sulfurtransferase in the brain. *Sci Rep* 5: 14774, 2015.
26. Marcolongo JP, Morzan UN, Zeida A, Scherlis DA, Olabe JA. Nitrosodisulfide [S<sub>2</sub>NO](-) (perthionitrite) is a true intermediate during the "cross-talk" of nitrosyl and sulfide. *Phys Chem Chem Phys* 18: 30047-30052, 2016.

27. Marcolongo JP, Venancio MF, Rocha WR, Doctorovich F, Olabe JA. NO/H<sub>2</sub>S "Crosstalk" Reactions. The Role of Thionitrites (SNO(-)) and Perthionitrites (SSNO(-)). *Inorg Chem* 58: 14981-14997, 2019.
28. Marcolongo JP, Zeida A, Slep LD, Olabe JA. Thionitrous Acid/Thionitrite and Perthionitrite Intermediates in the "Crosstalk" of NO and H<sub>2</sub>S. *Adv Inorg Chem* 70: 277-309, 2017.
29. Martinsen A, Songstad J. Preparation and Properties of Some Bis(Triphenylphosphine)-Iminium Salts, [(Ph<sub>3</sub>p)<sub>2</sub>n]X. *Acta Chem Scand A* 31: 645-650, 1977.
30. Mishanina TV, Libiad M, Banerjee R. Biogenesis of reactive sulfur species for signaling by hydrogen sulfide oxidation pathways. *Nat Chem Biol* 11: 457-64, 2015.
31. Miyamoto R, Koike S, Takano Y, Shibuya N, Kimura Y, Hanaoka K, Urano Y, Ogasawara Y, Kimura H. Polysulfides (H<sub>2</sub>Sn) produced from the interaction of hydrogen sulfide (H<sub>2</sub>S) and nitric oxide (NO) activate TRPA1 channels. *Sci Rep* 7: 45995, 2017.
32. Mustafa AK, Gadalla MM, Sen N, Kim S, Mu WT, Gazi SK, Barrow RK, Yang GD, Wang R, Snyder SH. H<sub>2</sub>S Signals Through Protein S-Sulfhydration. *Sci Signal* 2, 2009.
33. Nagy P, Palinkas Z, Nagy A, Budai B, Toth I, Vasas A. Chemical aspects of hydrogen sulfide measurements in physiological samples. *Biochim Biophys Acta* 1840: 876-91, 2014.
34. Ruff JK, Schlientz WJ, Dessy RE, Malm JM, Dobson GR, Memering MN.  $\mu$ -Nitridobis(triphenylphosphorus)(I+) ("PPN") Salts with Metal Carbonyl Anions. In: *Inorganic Syntheses*. 1974. pp. 84-90.
35. Seel F, Kuhn R, Simon G, Wagner M, Krebs B, Dartmann M. Pnp-Perthionitrite and Pnp-Monothionitrite. *Zeitschrift Fur Naturforschung Section B-a Journal of Chemical Sciences* 40: 1607-1617, 1985.
36. Stenger B, Popp T, John H, Siegert M, Tsoutsoulopoulos A, Schmidt A, Muckter H, Gudermann T, Thiermann H, Steinritz D. N-Acetyl-L-cysteine inhibits sulfur mustard-induced and TRPA1-dependent calcium influx. *Arch Toxicol* 91: 2179-2189, 2017.

37. Sutton T, Minnion M, Barbarino F, Koster G, Fernandez B, Cumpstey A, Wischmann P, Madhani M, Frenneaux M, Postle T, Cortese-Krott MM, Feelisch M. A robust and versatile mass spectrometry platform for comprehensive assessment of the thiol redox metabolome. *Redox Biol* 16: 359-380, 2018.
38. Szabo C. A timeline of hydrogen sulfide (H<sub>2</sub>S) research: From environmental toxin to biological mediator. *Biochem Pharmacol* 149: 5-19, 2018.
39. Wallace JL, Wang R. Hydrogen sulfide-based therapeutics: exploiting a unique but ubiquitous gasotransmitter. *Nat Rev Drug Discov* 14: 329-45, 2015.
40. Wang R. Physiological implications of hydrogen sulfide: a whiff exploration that blossomed. *Physiol Rev* 92: 791-896, 2012.
41. Wedmann R, Ivanovic-Burmazovic I, Filipovic MR. Nitrosopersulfide (SSNO(-)) decomposes in the presence of sulfide, cyanide or glutathione to give HSNO/SNO(-): consequences for the assumed role in cell signalling. *Interface Focus* 7: 20160139, 2017.
42. Wedmann R, Zahl A, Shubina TE, Durr M, Heinemann FW, Bugenhagen BE, Burger P, Ivanovic-Burmazovic I, Filipovic MR. Does perthionitrite (SSNO(-)) account for sustained bioactivity of NO? A (bio)chemical characterization. *Inorg Chem* 54: 9367-80, 2015.
43. Whiteman M, Li L, Kostetski I, Chu SH, Siau JL, Bhatia M, Moore PK. Evidence for the formation of a novel nitrosothiol from the gaseous mediators nitric oxide and hydrogen sulphide. *Biochem Biophys Res Commun* 343: 303-10, 2006.
44. Williams DL. S-nitrosothiols and role of metal ions in decomposition to nitric oxide. *Methods Enzymol* 268: 299-308, 1996.
45. Zhang D, Macinkovic I, Devarie-Baez NO, Pan J, Park CM, Carroll KS, Filipovic MR, Xian M. Detection of protein S-sulfhydration by a tag-switch technique. *Angew Chem Int Ed Engl* 53: 575-81, 2014.

## Figure legends

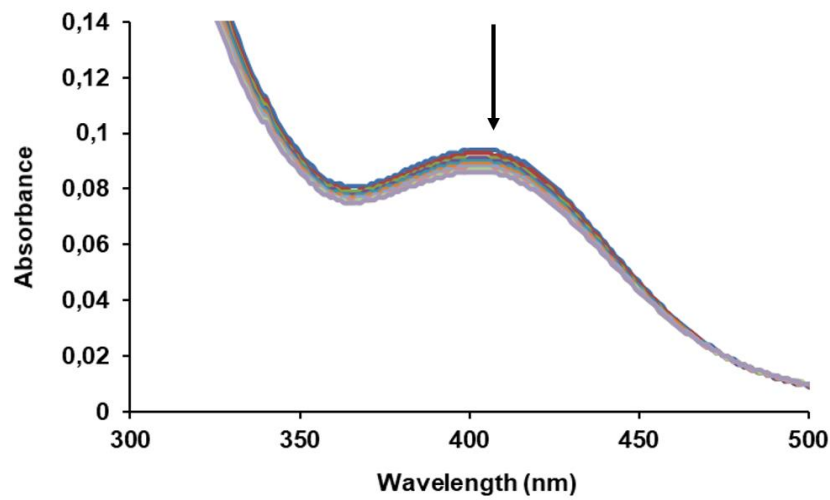


**Figure 1: Spectral changes of PNP<sup>+</sup>SSNO<sup>-</sup> in the presence of sulfide.** 0.52 mg (164  $\mu$ M) PNP<sup>+</sup>SSNO<sup>-</sup> was dissolved in 1 ml DMSO, then diluted to 5 ml in 100 mM phosphate buffer containing 1 mM sulfide. Spectra were recorded in every 30 s for 5 min, a slow absorbance decrease was observed at 412 nm. For more details please see Materials and Methods.

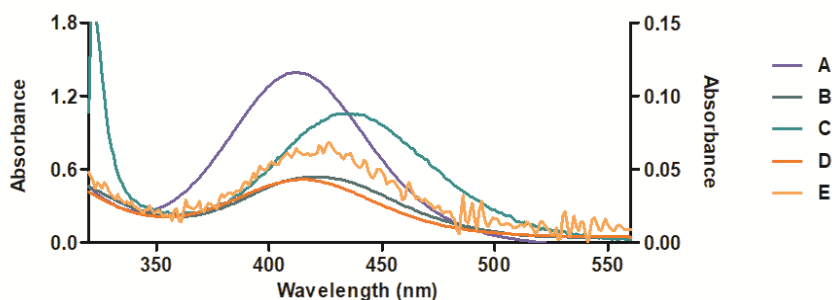


**Figure 2: UV-Vis spectral changes observed after preparation of SSNO<sup>-</sup> in aqueous media followed by dilution with acetone and methanol.** SSNO<sup>-</sup> was prepared by mixing 1 mM SNAP and 10 mM sulfide in Tris/HCl buffer, pH = 7.40. The observed  $\lambda_{\max}$  values were found to be located at 412 nm in aqueous media (A), 418 nm in 50% Tris/HCl buffer–50 % acetone (B), 439 nm in 10% Tris/HCl buffer–90% acetone (C), 415 nm in 50% Tris/HCl buffer–50 % MeOH (D) and 426 nm in 10% Tris/HCl buffer–90 % MeOH (E), respectively. Spectra A, B and D are attributed to the left Y axis, whereas absorbance value of spectra C and E correspond to the right Y axis. For more details please see Materials and Methods.

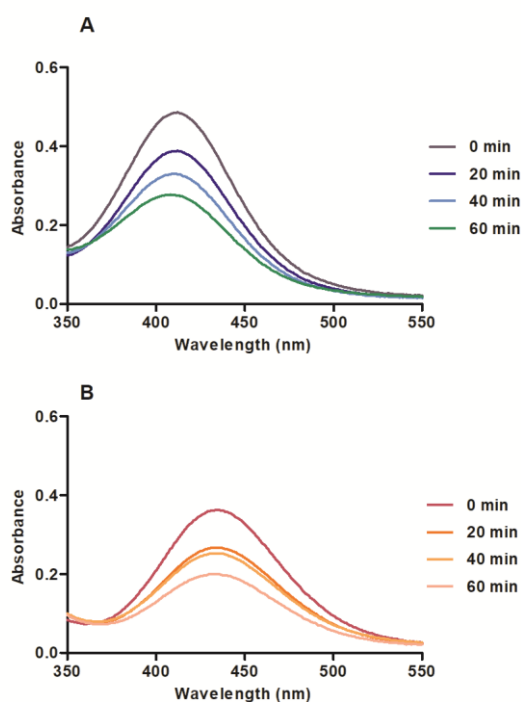


**Figure 3: UV-Vis spectral changes observed during the kinetic study of SSNO<sup>-</sup> decomposition.** SSNO<sup>-</sup> was prepared by mixing 3 mM SNAP and 30 mM sulfide in Tris/HCl buffer, pH = 7.40. The majority of preformed inorganic polysulfides were eliminated by a reductant column activated by 10 mM DTT. Decomposition of SSNO<sup>-</sup> (the “412 species”) was followed by taking aliquots from the reaction mixture at the indicated timepoints, which were diluted 10 times in A) 200 mM Tris/HCl buffer and B) acetone before recording UV-Vis spectra. Figures are representative of n = 3 independent experiments with similar results. For more details please see Materials and Methods.

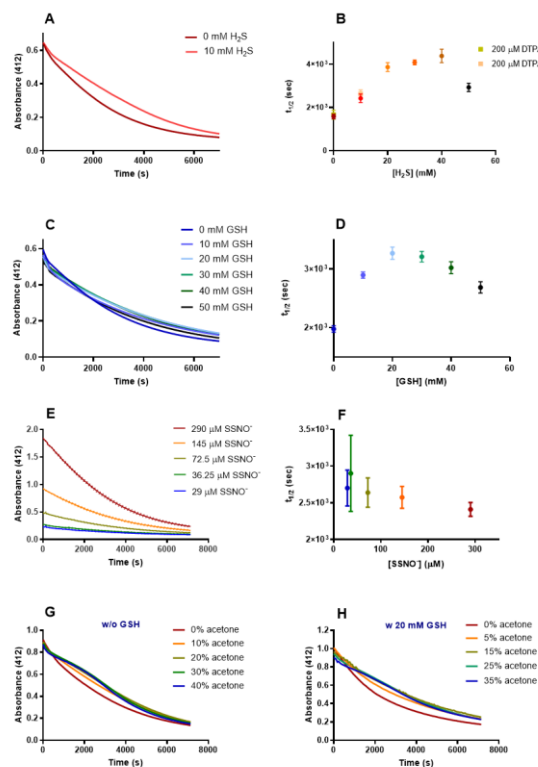


**Figure 4: Decomposition kinetics of  $\text{SSNO}^-$ .** Decomposition of  $\text{SSNO}^-$  under different conditions was monitored using UV-Vis spectrometry at 412 nm in 200mM Tris/HCl buffer pH 7.40. The majority of the generated inorganic polysulfides and the residual sulfide were eliminated using 100 nM TrxR1 and 1 mM NADPH and by degassing with  $\text{N}_2$ , respectively. Half-lives were calculated from exponential fittings of the kinetic curves. For more details please see Materials and Methods.

**A)** Kinetic traces for the decomposition of 308  $\mu\text{M}$   $\text{SSNO}^-$  in the presence or absence of  $\text{H}_2\text{S}$  (0-50mM). **B)** Measured half-lives of  $\text{SSNO}^-$  as a function of the concentration of  $\text{H}_2\text{S}$  in the solution. Colors of points correspond to the colors of traces in panel A. At 0 and 10 mM sulfide the experiments were conducted both at the presence (squares) and absence (filled circles) of 200  $\mu\text{M}$  DTPA. Overlapping  $t_{1/2}$  values indicate no effect of this metal chelator on the decomposition kinetics of  $\text{SSNO}^-$ . **C)** Kinetic traces for the decomposition of 266  $\mu\text{M}$   $\text{SSNO}^-$  in the presence or absence of GSH (0-50mM). **D)** Measured half-lives of  $\text{SSNO}^-$  as a function of the concentration of GSH in the solution. Colors of points correspond to the colors of traces in panel C. **E)** Kinetic traces for the decomposition of  $\text{SSNO}^-$  at different starting concentrations in the range of 29-290  $\mu\text{M}$   $\text{SSNO}^-$ . A 290  $\mu\text{M}$  stock solution was diluted with 200mM Tris/HCl just before measurement. **F)** Measured

half-lives of  $\text{SSNO}^-$  decomposition after dilution. Colors of points correspond to the colors of traces in panel E. **G)** Kinetic traces for the decomposition of  $290 \mu\text{M SSNO}^-$  as a function of the acetone content of the media (0-40%) in the absence of GSH. Optical pathlength correction was carried out using acetone-buffer mixtures to determine the appropriate correction factors. **H)** Kinetic traces for the decomposition of  $340 \mu\text{M SSNO}^-$  as a function of the acetone content of the media (0-35%) in the presence of 20 mM GSH. Optical pathlength correction was carried out using acetone-buffer mixtures to determine the appropriate correction factors. Kinetic traces on Figures 4A, C, E, G and H are representative of  $n = 3$ , respectively and data points and error bars on Figs 4 B, D and F represent average values and standard deviations of  $n = 3$  independent experiments.



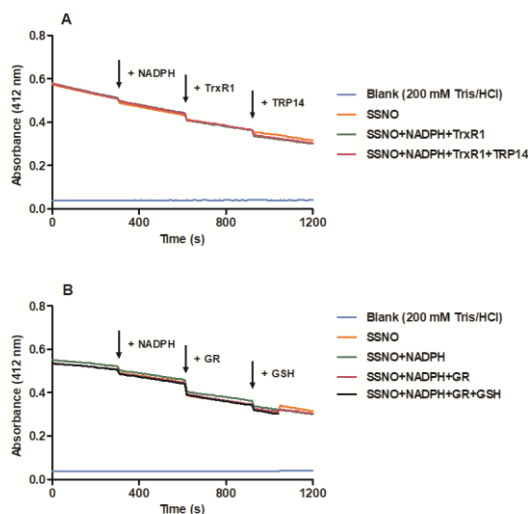


**Figure 5.: Kinetic traces for the effects of the enzymatic thioredoxin (A) and glutathion (B) reductase systems on the decomposition of SSNO<sup>-</sup>.** Addition of 500  $\mu$ M NADPH, even in the presence of 100 nM TrxR1, 2  $\mu$ M TRP14 (A) or 100 nM GR, 1 mM GSH (B) had no effect on the kinetics of the slow decomposition of SSNO<sup>-</sup> (prepared by the reaction of 1 mM SNAP and 10 mM sulfide). The different components of the NADPH reducing systems were added where indicated by the arrows. Figures are representative of  $n = 3$  independent experiments with similar results. For more details please see Materials and Methods.

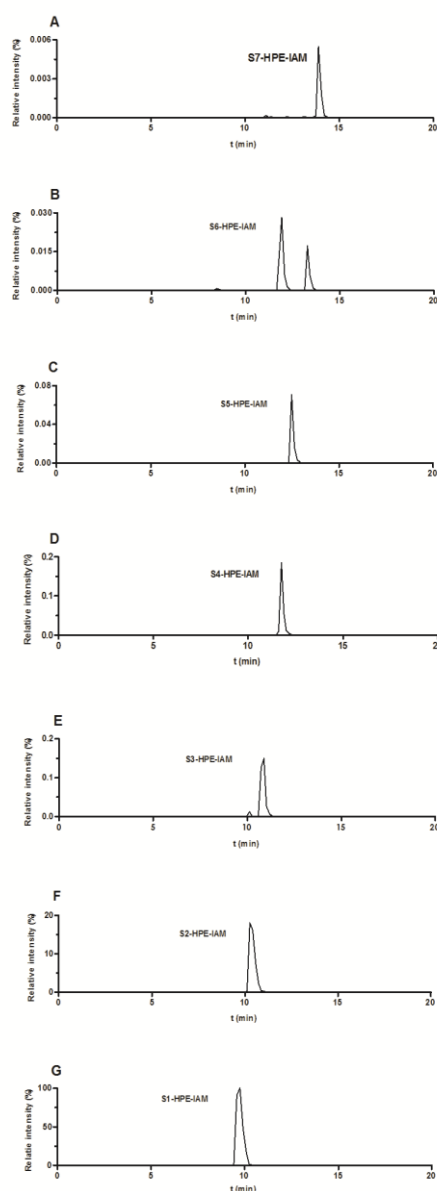


**Figure 6: LC-MS/MS analysis of inorganic polysulfide – HPE-IAM adducts following SSNO<sup>-</sup> decomposition. (A-G)** HS<sub>n</sub>-HPE-IAM (n=1-7) adducts were detected in the reaction mixture of 1 mM SNAP and 10 mM sulfide in 200 mM Tris/HCl buffer, pH = 7.40 (purified from the majority of preformed inorganic polysulfides with 2 mM NADPH and 200 nM TrxR1) after 120 min incubation in the dark followed by alkylation of polysulfide species with 25 mM HPE-IAM for 30 min, all at RT. Detection and quantitation of the species was carried out using the SRM detection parameters of Table 1. The data depicted in Figure 6 is representative of n = 3 independent experiments with similar results.

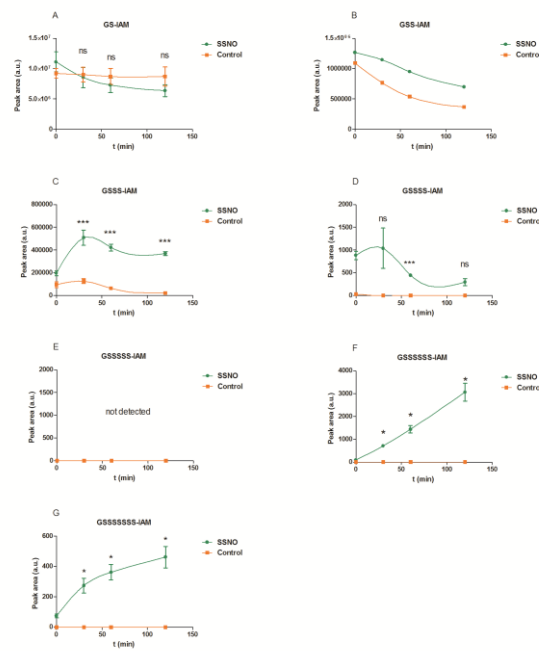


**Figure 7: Sustained polysulfidation of GSH upon SSNO<sup>-</sup> treatment.** Significantly more polysulfidated GS(S)<sub>n</sub> species (**B-G**) were detected in samples where GSH was treated with SSNO<sup>-</sup> compared to control samples at all timepoints. Interestingly, a steady increase of longer-chain glutathione-polysulfur species (**F** and **G**) was observed when GSH was treated with SSNO<sup>-</sup>, which was not seen in control samples. Solid lines on the graphs are fitted cubic spline functions only to indicate trends between the individual data points. Data points represent the average of n=3 independent experiments with the corresponding error bars showing the SD (3 different experiments were performed on 3 independent days under identical conditions). All peak areas in each sample are relative values to those measured for GSS-IAM (set at the average of n = 3, Panel B). ns = P ≥ 0.05, \* = 0.01 ≤ P < 0.05, \*\* = 0.001 ≤ P < 0.01, \*\*\* = P < 0.001.

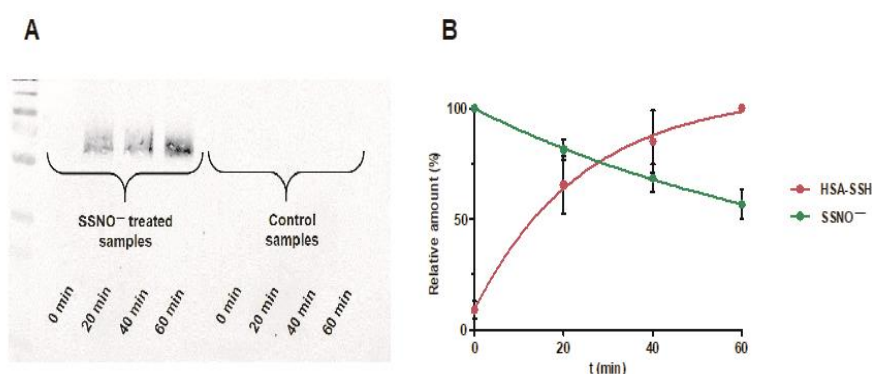


**Figure 8: Time resolved polysulfidation of HSA by inorganic polysulfides that are generated upon SSNO<sup>-</sup> decomposition.**

**A)** Exemplary western blot represents increasing amounts of HSA–SSH, generated during the reaction of Cys34 of HSA with purified SSNO<sup>-</sup>. Control samples, which were treated with a mixture containing 9 mM Na<sub>2</sub>S and 500 μM Na<sub>2</sub>S<sub>2</sub> (after a similar dilution to the SSNO<sup>-</sup> stock solutions to represent the preformed inorganic polysulfide and sulfide content of working SSNO<sup>-</sup> solution) were subjected to the same enzymatic purification and sulfide removal process as the SSNO<sup>-</sup> preparation, did not contain any detectable amount of HSA–SSH. Figure is representative of n = 3 different experiments with similar results, performed on three independent days under identical conditions. For more details see text and Materials and Methods.

**B)** The kinetics of HSA-SSH formation upon treatment with SSNO<sup>-</sup> is consistent with the kinetics of SSNO<sup>-</sup> decomposition, corroborating that persulfidation of HSA is caused by inorganic polysulfides generated during SSNO<sup>-</sup> decomposition. HSA-SSH formation was detected by the ProPerDP method and SSNO<sup>-</sup> decomposition was monitored by UV-Vis spectroscopy under similar conditions (see Materials and Methods). Data points represent the average of n = 3 independent experiments with the corresponding error bars showing the SD. (Three different experiments were performed on three independent days under identical conditions).

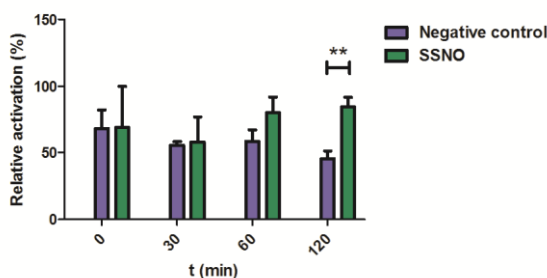


**Figure 9: Time dependent activation of TRPA1 expressing CHO cells**

Processed GSNO/sulfide mixtures were diluted to a nominal concentration of  $10 \mu\text{M}$   $\text{SSNO}^-$  at  $t=0$ . The same dilution factor was then used for all other time points. As a control sample, a solution containing  $9 \text{ mM Na}_2\text{S} + 0.5 \text{ M Na}_2\text{S}_2$  was prepared, purified and allowed to decompose in parallel with  $\text{SSNO}^-$  to demonstrate the effects of residual inorganic polysulfides and sulfide at  $t=0$  (due to incomplete enzymatic reduction of polysulfides and removal of sulfide by bubbling with  $\text{N}_2$ ). As positive control, cell groups were reacted with the selective TRPA1 receptor agonist mustard-oil ( $100 \mu\text{M}$  in ECS). Observed fluorescence in positive control samples was set as 100%. Data points represent the average of  $n = 3$  independent experiments with the corresponding error bars showing the SD. (Three different experiments were performed on three independent days under identical conditions).  $** = 0.001 \leq P < 0.01$ .

## Supporting Information

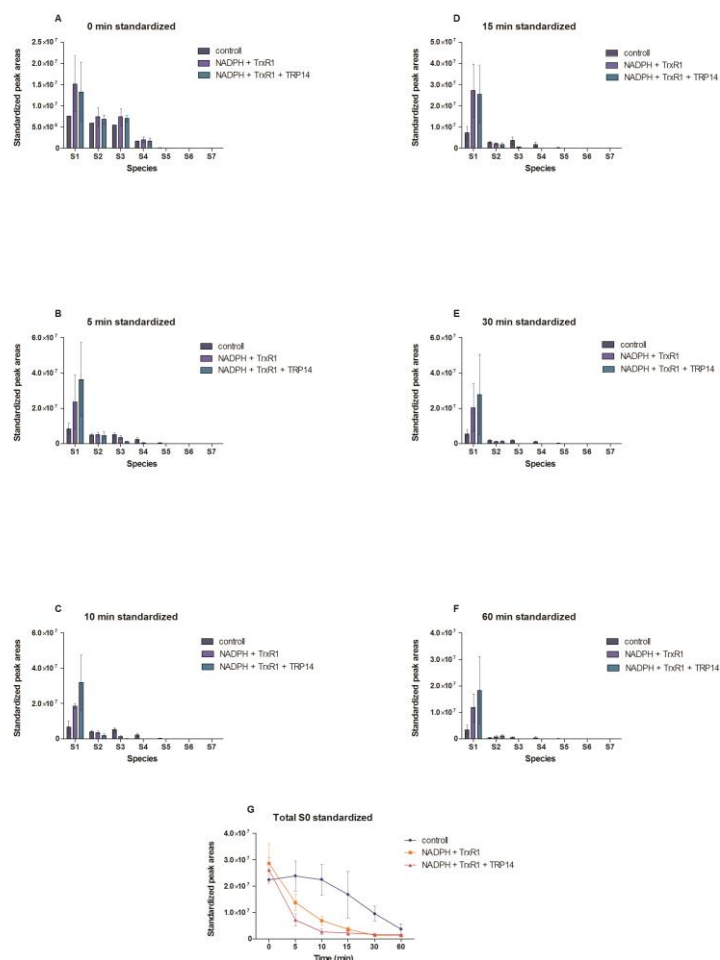


**Figure S1: Enzymatic reduction of 100  $\mu\text{M}$   $\text{Na}_2\text{S}_2$  by the NADPH-TrxR1-TRP14 system.**

The bar graphs (A-E) show the changes in inorganic polysulfide levels at the indicated time points in the absence (dark violet bars) or presence of 250  $\mu\text{M}$  NADPH and 100 nM TrxR1 (blue bars) or 250  $\mu\text{M}$  NADPH, 100 nM TrxR1 and 2  $\mu\text{M}$  TRP14 (green bars). The time resolved demonstration for the changes in total inorganic polysulfide species represents the sum of the relative intensities in the LC-MS (single ion monitoring) chromatograms. Due to potential differences in the ionization of the different chain length polysulfides as well as ion suppression problems that were not accounted for by using isotopically labelled internal standards, this data should not be considered quantitative. In panel (F) the orange line corresponds to the enzymatic reduction of 100  $\mu\text{M}$   $\text{Na}_2\text{S}_2$  by 250  $\mu\text{M}$  NADPH in the presence of 100 nM TrxR1, the violet line shows the enzymatic reduction of 100  $\mu\text{M}$   $\text{Na}_2\text{S}_2$  by 100 nM TrxR1 and 2  $\mu\text{M}$  TRP14. The blue line represents the control samples,

containing only 100  $\mu\text{M}$   $\text{Na}_2\text{S}_2$ . Values and error bars represent the averages and standard deviations of 3 independent experiments.

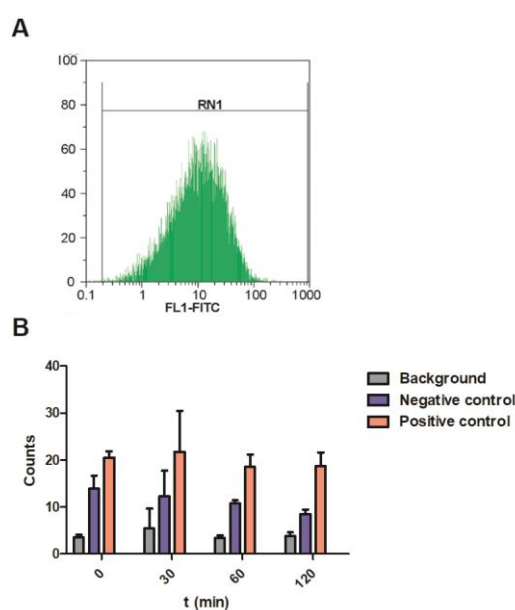


**Figure S2:** Representative flow cytometry recording of Fluo-4 stained TRPA1 expressing CHO cells (A) and time dependent activation of TRPA1 expressing CHO cells (B).

(A) Representative flow cytometry recording of Fluo-4 stained TRPA1 expressing CHO cells. X axis refers to fluorescent signal, Y axis represents the number of cells reacted. Mean fluorescence refers to the fluorescent signal divided by the number of cells. Increased intracellular  $\text{Ca}^{2+}$  levels resulted in higher mean values due to increased fluorescence.

(B) Mean green fluorescence values of cell groups reacted with ECS buffer (background), a solution containing 9 mM  $\text{Na}_2\text{S}$  + 0.5 M  $\text{Na}_2\text{S}_2$ , purified and allowed to decompose in parallel with  $\text{SSNO}^-$  to demonstrate the effects of residual inorganic polysulfides and sulfide at t=0 (due to incomplete enzymatic reduction of polysulfides and removal of sulfide by bubbling with  $\text{N}_2$ , negative control) and the selective TRPA1 receptor agonist mustard-oil (100  $\mu\text{M}$  in ECS, positive control) and analyzed by flow cytometry immediately.



**Tables**

Table 1: Parameters for MS/MS detection of the HPE-IAM labeled inorganic polysulfide species.

Species	Parent ion (m/z)	Fragment (m/z)
HS <sup>-</sup>	389	252
HSS <sup>-</sup>	421	212
HSSS <sup>-</sup>	453	244
HSSSS <sup>-</sup>	485	276
HSSSSS <sup>-</sup>	517	308
HSSSSSS <sup>-</sup>	549	485
HSSSSSSS <sup>-</sup>	581	454